OPTIMIZATION OF THE GAIN-BANDWIDTH PRODUCT OF CAPACITIVE MICROMACHINED ULTRASONIC TRANSDUCERS

A THESIS

SUBMITTED TO THE DEPARTMENT OF ELECTRICAL AND

ELECTRONICS ENGINEERING

AND THE INSTITUTE OF ENGINEERING AND SCIENCE

OF BILKENT UNIVERSITY

IN PARTIAL FULFILLMENT OF THE REQUIREMENTS

FOR THE DEGREE OF

MASTER OF SCIENCE

By

Selim Olçum

January, 2005

I certify that I have read this thesis and that in my opinion it is fully adequate, in scope and in quality, as a thesis for the degree of Master of Science.

Prof. Dr. Abdullah Atalar(Supervisor)

I certify that I have read this thesis and that in my opinion it is fully adequate, in scope and in quality, as a thesis for the degree of Master of Science.

Prof. Dr. Hayrettin Köymen

I certify that I have read this thesis and that in my opinion it is fully adequate, in scope and in quality, as a thesis for the degree of Master of Science.

Assoc. Prof. Dr. Ahmet Oral

Approved for the Institute of Engineering and Science:

Prof. Dr. Mehmet Baray
Director of the Institute Engineering and Science

ABSTRACT

OPTIMIZATION OF THE GAIN-BANDWIDTH PRODUCT OF CAPACITIVE MICROMACHINED ULTRASONIC TRANSDUCERS

Selim Olçum
M.S. in Electrical and Electronics Engineering
Supervisor: Prof. Dr. Abdullah Atalar
January, 2005

Capacitive micromachined ultrasonic transducers (cMUT) have large bandwidths, but they typically have low conversion efficiencies. This thesis defines a performance measure in the form of a gain-bandwidth product, and investigates the conditions in which this performance measure is maximized. A Mason model corrected with finite element simulations is utilized for the purpose of optimizing parameters. There are different performance measures for transducers operating in transmit, receive or pulse-echo modes. Basic parameters of the transducer are optimized for those operating modes. Optimized values for a cMUT with silicon nitride membrane and immersed in water are given. The effect of including an electrical matching network is considered. In particular, the effect of a shunt inductor in the gain-bandwidth product is investigated. Design tools are introduced, which are used to determine optimal dimensions of cMUTs with the specified frequency or gain response.

Keywords: Capacitive Micromachined Ultrasonic Transducers (cMUT), Transducer Gain, Bandwidth.

ÖZET

KAPASİTİF MİKRO-İŞLENMİŞ ULTRASONİK ÇEVİRGEÇLERİN KAZANÇ-BAND GENİŞLİĞİ ÇARPIMLARININ OPTİMİZASYONU

Selim Olçum
Elektrik Elektronik Mühendisliği, Yüksek Lisans
Tez Yöneticisi: Prof Dr. Abdullah Atalar
Ocak, 2005

Kapasitif Mikroişlenmiş Ultrasonik Çeviriciler (kMUÇ) geniş bantlı üretilebilmelerine rağmen, düşük çevrim verimliliğine sahiplerdir. Bu çalışmada, kMUÇ cihazları için yeni bir başarım ölçüsü, kazanç-bant genişliği çarpımı olarak tanımlanmıştır. Bu başarım ölçüsünü en yüksek değere çıkarmak için gereken ölçütler araştırılmıştır. Üretim parametrelerini eniyileştirmek amacıyla Mason'ın eşdeğer devre modeli kullanılmış ve bu modelden elde edilen sonuçlar sonlu eleman metodu kullanılarak düzeltilmiştir. kMUÇ cihazları, iletici, almaç ve darbe-yankı modlarında çalıştırılırken, farklı başarım ölçütleri tanımlanmalıdır. kMUÇ cihazlarının temel parametreleri bu üç çalışma modu için eniyileştirilmiştir. Bu çalışmada, su içerisinde çalışan, silikon nitrat bir zara sahip kMUÇ cihazları için en iyi üretim değerleri saptanmıştır. Elektriksel bir eşleştirme devresinin etkileri incelenmiştir. Özellikle bir paralel endüktansın kazanç-bant genişliği çarpımına olan etkisi incelenmiştir. İstenilen özelliklere sahip bir kMUÇ cihazı üretebilmek için gereken tasarım gereçleri sunulmuştur.

Anahtar sözcükler: Kapasitif Mikro-işlenmiş Ultrasonik Çevirici (kMUÇ), çevirici kazancı, bant genişliği.

Acknowledgement

I am sincerely grateful to Prof. Abdullah Atalar for his supervision, guidance and valuable suggestions throughout the development of this thesis.

Thanks to Niyazi for valuable discussions and being around at late working nights. He was my teacher for FEM simulations.

Many thanks to my parents, my brother and Gökçe for their loving support and being with me all the time.

Contents

List of Figures

Chapter 1

Introduction

Capacitive micromachined ultrasonic transducers (cMUTs) [1–3] have the potential of replacing piezoelectric transducers in many areas. The applications include air-coupled nondestructive testing [4, 5], medical imaging [6, 7], 3D immersion imaging with 2D transducer arrays [8], flow meters, level meters, position and distance measurements and microphones. Recently, analytical and computational models for the cMUTs have been developed [9–12]. Drawbacks of the cMUTs are studied and eliminated for optimum performance for a variety of applications. Increasing the dynamic range, decreasing parasitic capacitances and cross-coupling [13] have been the major goals. The methods to overcome the problems include new ways of electrode patterning [14, 15], changing the material used for membrane, optimizing the geometry for the best operation [16].

There are several processes utilized in the fabrication of the cMUTs [10, 17–23]. In this study, the transducers are assumed to be fabricated with the process in [17]. The process utilizes polysilicon as a sacrificial layer. The ground electrode insulator, stand region and the membrane are all fabricated from silicon nitride by LPCVD. All of the analyses in this study assume that the transducers are fabricated in circular shape, since both the analytical model and FEM simulations are easily computed.

It is shown that a large bandwidth is possible with an untuned cMUT immersed in water [10, 14]. For such a cMUT the operation frequency range may extend from

very low frequencies to the antiresonance of the membrane [24]. However, those cMUTs have small conversion efficiencies and are not as sensitive as piezoelectric transducers. An electrical tuning network can be added to increase the gain. In this work, we explore the limits of a cMUT operating in different regimes using the Mason model corrected with finite element method (FEM) simulations. We try to maximize the bandwidth of a cMUT while keeping the output pressure or the conversion efficiency at a reasonable value. For this purpose, we define performance measures in the form of a pressure-bandwidth product or a gain-bandwidth product. We try to maximize this figure of merit by optimizing various geometrical parameters of the cMUT.

We have two main objectives. The first one is to develop fast and accurate results by modelling the transducers with an electrical circuit. Mason's lumped equivalent circuit model, which is discussed in the following chapter, is used for simulating the operation of a cMUT. The analytical modelling of cMUTs are based on the previous studies [3,10,12,14,17,25,26]. The parameters calculated by the analytical results are modified with FEM simulations which are based on the methods developed in [14]. The second objective is to characterize and optimize cMUTs for different operating regimes and for different design parameters. The tools for designing a cMUT with specified frequency response are introduced.

Chapter 2

Electrical Modelling of cMUTs

Usually the analysis of a cMUT is based on the lumped equivalent circuit approach [27]. In the previous studies about cMUTs, Mason's equivalent circuit in Fig. 2.1 is utilized [2, 10, 11, 14, 24, 26, 28]. In Fig. 2.1, C_0 is the shunt input capacitance, n_c is the transformer ratio, Z_m is the lumped mechanical impedance of the membrane, S is the area of the membrane and Z_a is the acoustical impedance of the medium.

The Mason's model consists of a mechanical port and an electrical port. The shunt input capacitance, C_0 in the electrical port is basically the capacitance between the top electrode and the ground electrode of the transducer. In the circuit model the electrical termination resistance, R_S is also taken into account.

The turns ratio (transformer ratio) of the transducer is the measure of how the acoustical signal at the mechanical port is transformed to the electrical signal or visa versa. The lumped mechanical impedance of the membrane, Z_m is approximated by the ratio of the applied uniform pressure on the membrane to the velocity of the membrane. Since the average velocity of the membrane is a function of the excitation frequency, Z_m is a function of frequency.

For a transmitter cMUT, the mechanical side of the circuit is terminated by the acoustical impedance of the medium. Acoustical impedance of a medium is defined

as the multiplication of the density of the medium with the velocity of the sound travels in the medium. In the case of water immersed applications, the acoustical impedance of water, Z_a is $1.5.10^6$ kg/m^{2}s.

In the previous studies, the mechanical impedance of the membrane is neglected with respect to the acoustical impedance of the immersion medium. In this case the equivalent circuit simplifies to an RC circuit. However, in this work we do not neglect the mechanical impedance and explored the effects of the device dimensions. In the case where mechanical impedance is not negligible, the gain of the transducer may be increased by a shunt tuning inductor. The effect of the tuning inductor is also investigated.

The parameters of the Mason's equivalent circuit is calculated using the MATLAB simulations[1] and FEM simulations[2]. The computation of the parameters in MATLAB environment is discussed in the next chapter.

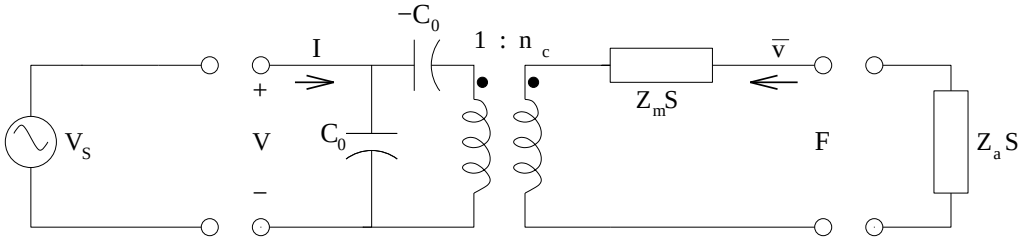

(a) Transmitter cMUT

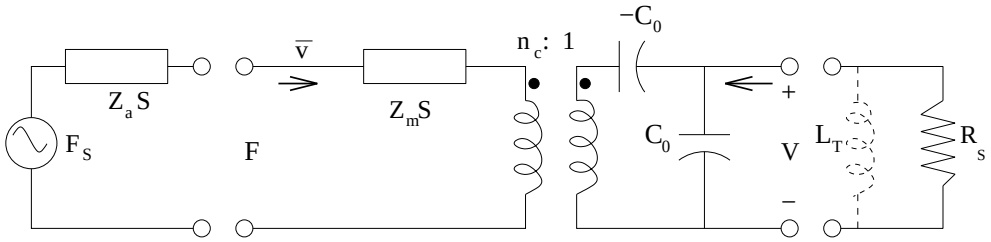

(b) Receiver cMUT

Figure 2.1: Mason model **(a)** for a cMUT operating as a transmitter excited by a voltage source (V_S) to drive the acoustic impedance of the immersion medium (Z_aS) **(b)** for a cMUT operating as a receiver excited by the acoustical source (F_S, Z_aS) to drive the electrical load resistance of the receiver circuitry (R_S). S is the area of the transducer, L_T is the tuning inductor.

[1]MATLAB Simulation codes are presented in Appendix E
[2]FEM Simulations are detailed in Appendix A

Chapter 3

Analytical Modelling of cMUTs

In order to find the characteristics of a cMUT for different dimensions (Fig. 3.1), we

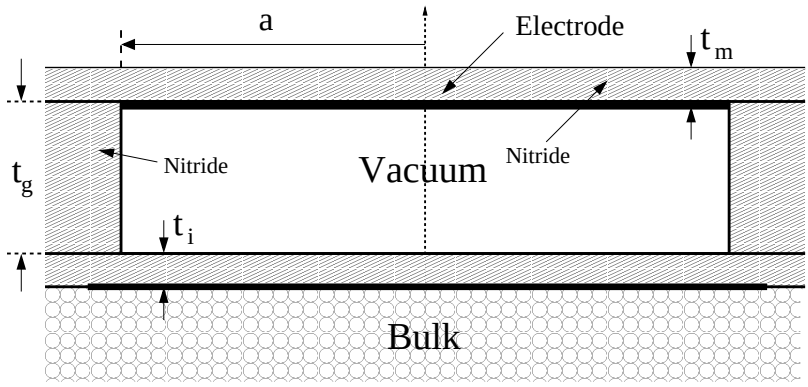

Figure 3.1: Cross sectional view of a cMUT.

should compute the electrical parameters in Fig. 2.1. In the previous studies, those parameters are calculated with FEM simulations. However, the computation time for FEM simulations is an obstacle to generate fast results. Therefore in this chapter, the electrical parameters are approximated by using their closed form expressions. However, the FEM results serve as a reference point in the analytical calculations.

The physical parameters of a cMUT can be seen at the cross sectional view in Fig. 3.1, where t_m is the thickness of the membrane, t_i is the thickness of the insulator on the bulk silicon. The radius of the membrane is represented by a and the gap height is symbolized by t_g. Other than the ground electrode, an electrode is

placed on the bottom of the membrane. All the cMUTs are assumed to be fabricated from silicon nitride with a top electrode at the bottom of the membrane.

3.1 Collapse Voltage

When the applied DC bias exceeds a critical value called collapse voltage, V_{col}, the membrane collapses onto the isolation layer. In order to make a fair comparison, all the transducers are simulated with 90% of the $Vcol$ is applied as DC bias. Since the collapse voltage determines the operating point of cMUTs, it is very critical to calculate this parameter accurately.

3.1.1 Parallel Plate Approximation

At the previous studies an approximate expression for the collapse voltage is derived [10, 14, 29], in which the transducer is assumed to be a parallel plate capacitor. The collapse voltage is calculated using the point where the restoring force of the membrane cannot overwhelm the electrostatic force. The resulting analytical expression is as follows;

$$V_{col} = \sqrt{\frac{128(Y_0 + T)t_m^3 \bar{t}_g^3}{27\epsilon_0(1-\sigma^2)a^4}} \tag{3.1}$$

where $\bar{t}_g$ is the effective gap height, $\bar{t}_g = t_g + \epsilon_0 t_i/\epsilon$. ϵ_0 and ϵ are the permittivity constants of air and insulation layer material respectively. Here, Y_0 is the Young's modulus, T is the residual stress and σ is the Poisson's ratio.

Because of the parallel plate approximation, Eq. 3.1 gives V_{col} values higher than FEM simulation does. If the analytical expression is multiplied by a factor of 0.7, the accuracy of the calculation increases considerably. Therefore, an approximate expression for the collapse voltage can be written as;

$$V_{col} \simeq 0.7\sqrt{\frac{128(Y_0 + T)t_m^3 \bar{t}_g^3}{27\epsilon_0(1-\sigma^2)a^4}} \tag{3.2}$$

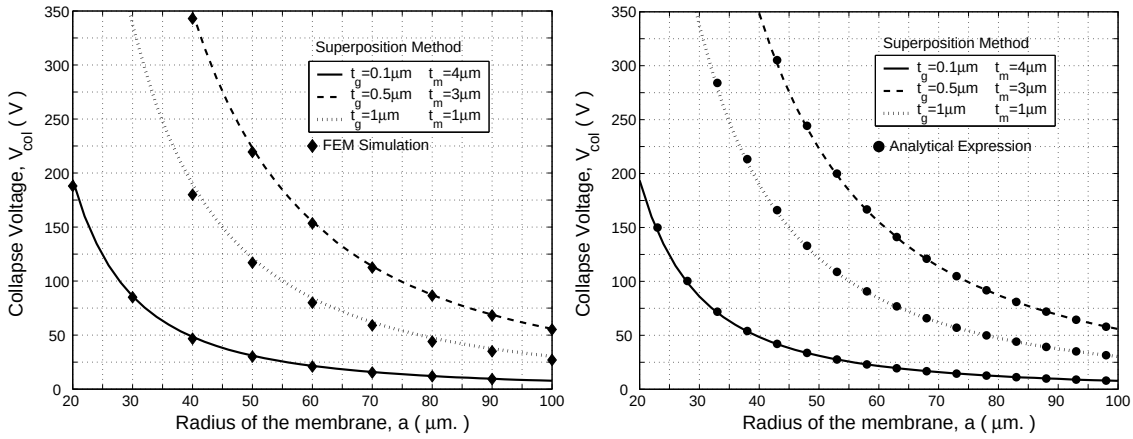

Figure 3.2: Collapse voltage of the cMUTs as a function of membrane radius, a, with t_m and t_g as parameters. V_{col} values are calculated by analytical expression, superposition method and FEM simulations. t_i is assumed to be 0. The top electrode is at the bottom of the membrane.

Note that this formulation assumes that the top electrode is placed at the bottom of the membrane. Eq. 5.1 gives the opportunity of calculating the collapse voltage of a transducer approximately, by using only hand calculations. However we need a more accurate model for determining the DC operating point of a membrane.

3.1.2 Superposition of Electrostatic Forces

A more accurate value for V_{col} can be determined using the method developed in [12]. In order to calculate the collapse voltage, we should calculate the deflection profile of the membrane when a particular DC voltage is applied. First we partition the membrane into nodes. The deflection profile for a corresponding node is calculated using the relations in [30];

$$x(r) = \sum_{i=1}^{N} \begin{cases} \frac{F_i}{8\pi D}\left[\frac{(a^2+r^2)(a^2-b_i^2)}{2a^2} + (b_i^2+r^2)ln\frac{b_i}{a}\right], & b_i < r; \\ \frac{F_i}{8\pi D}\left[\frac{(a^2-r^2)(a^2+b_i^2)}{2a^2} + (b_i^2+r^2)ln\frac{r}{a}\right], & b_i \geq r. \end{cases} \tag{3.3}$$

where F_i is the electrostatic force between the electrodes at the i^{th} node, D is the flexural rigidity of the membrane which is equal to, $\frac{Et_m^3}{12(1-\sigma^2)}$, r is the axial distance

of the corresponding node to the center node and b_i is the axial distance of force F_i to the center node.

After finding the first deflection with superposition, we should continue our calculation iteratively updating the gap, t_g, —thus electrostatic forces, F_i— until the deflection converges. If the result of the iterations does not converge, the applied voltage is decreased and the same method is utilized again.

A fast line search algorithm is implemented in a predefined tolerance (0.1V), to find the maximum voltage value that does not make the deflection diverge. We determine V_{col} and the deflection profile, $x(r)$, of the membrane for DC biased operation. The resulting V_{col} values are within 5% of the results obtained with FEM simulations.

In Fig. 3.2, the results of the collapse voltage calculations with three different methods are compared. We note that both the analytical calculations and the superposition method are in harmony with the FEM simulation results.

3.2 Input Capacitance

Another electrical parameter that depends on the physical dimensions is the shunt input capacitance at the electrical port. Basically, this capacitance is the capacitance between the ground electrode and the top (membrane) electrode. The value of this capacitance can be found by the parallel plate approximation [29]

$$C_0 \simeq 2\pi\epsilon_0 \int_0^{a+\bar{t}_g} \frac{r}{\bar{t}_g - x(r)} dr \tag{3.4}$$

where $x(r)$ is the deflection profile of the membrane as determined by the superposition method. The extra capacitance due to fringing fields is included approximately by extending the radius from a to $a+\bar{t}_g$. The accuracy of the model is tested for the gap height values between 0.1 μm and 1 μm. The resulting capacitance values are within 1% of the corresponding FEM simulations. The comparison of the results with the FEM simulations is demonstrated in Fig. 3.3. Note that the membrane

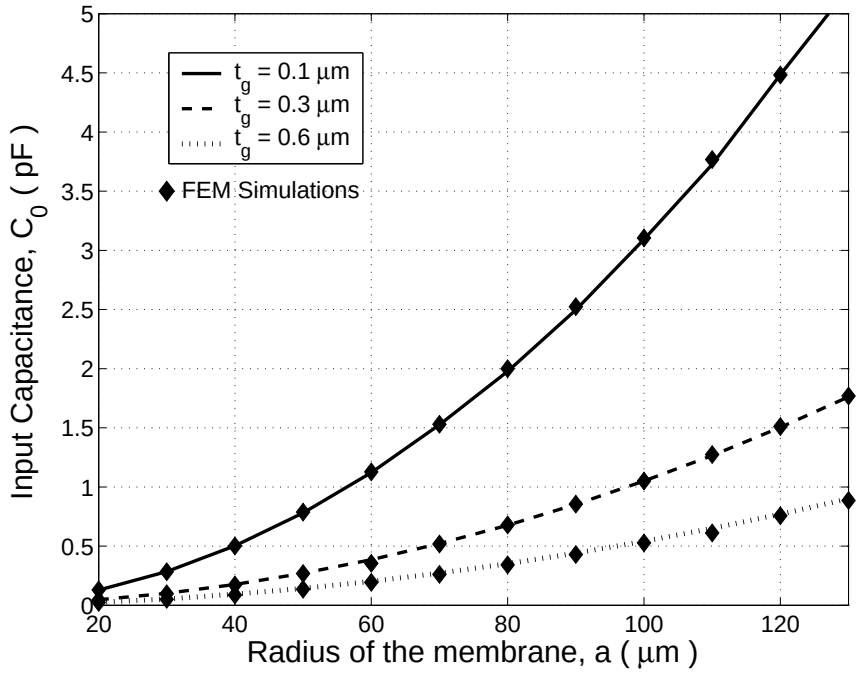

Figure 3.3: Shunt input capacitance, C_0 as a function of membrane radius, a, with gap height, t_g as a parameter. Results are calculated analytically (solid,dashed,dotted) and with FEM simulations (diamond). $V_{DC} = 0.9V_{col}$. Insulation layer thickness, t_i=0. The results are independent of the membrane thickness, t_m.

thickness, t_m, does not affect the value of C_0, since the electrode is placed at the bottom of the membrane.

Typically, many cMUT cells are connected together to form a transducer. An extra capacitance called spurious capacitance arises because of the interconnections between the cMUT electrodes. Since this capacitance can be quite large, the effect of presenting spurious capacitance is also investigated in Chapter 4.

3.3 Turns Ratio

After the membrane is deflected by a DC bias, the cMUTs are operated under a harmonic voltage excitation between its electrodes. The total voltage applied on the

top electrode during the transmission is;

$$V(t) = V_{DC} + V_{AC}cos(\omega t + \phi) \tag{3.5}$$

Since the corresponding electrostatic force when the potential of V applied between the electrodes is;

$$F = \frac{1}{2}\epsilon_0 S \frac{V^2}{(\bar{t_g} - x(r))^2} \tag{3.6}$$

the total force corresponding to the total applied voltage in Eq. 3.5 is;

$$F = \frac{\epsilon_0 S}{2\,(\bar{t_g} - x(r))^2}\left(V_{DC}^2 + 2V_{DC}V_{AC}cos(\omega t + \phi) + V_{AC}^2 cos^2(\omega t + \phi)\right) \tag{3.7}$$

If $V_{DC} \gg V_{AC}$, the time varying force on the membrane is approximated by;

$$F_{AC} \simeq \frac{\epsilon_0 S V_{DC} V_{AC}}{(\bar{t_g} - x(r))^2} cos\left(\omega t + \phi\right)) \tag{3.8}$$

Referring to the Mason's equivalent circuit in Fig. 2.1, the turns ratio is the ratio of the force at the mechanical side to the applied voltage on the electrical side. Therefore, using Eq. 3.8 we can calculate the turns ratio of the equivalent circuit as;

$$n \simeq \frac{F_{AC}}{V_{AC}} = \frac{\epsilon_0 S V_{DC}}{(\bar{t_g} - x(r))^2} = C_0 E \tag{3.9}$$

where E is the electric field between the ground electrode and deflected membrane electrode.

This calculation assumes that the AC signal is much smaller than the DC bias. In the FEM simulations used during this work the AC voltage is taken to be the 1% of the collapse voltage, thus the AC signal is 1.11% of the applied DC bias.

As it is seen in Eq. 3.9, the turns ratio, n is calculated as the product of the capacitance with the electric field, for small AC deflections of the membrane. In order to take into account the fringing fields, corrected turns ratio, n_c for a deflected membrane can be determined by the following integration:

$$n_c \simeq 2\pi\epsilon_0 V_{DC} \int_0^{a+\bar{t}_g} \frac{r}{(\bar{t}_g - x(r))^2} dr \tag{3.10}$$

This calculation holds true as long as the deflection of the membrane because of the small voltage changes is small. In Fig. 3.4, the sensitivity of the membrane

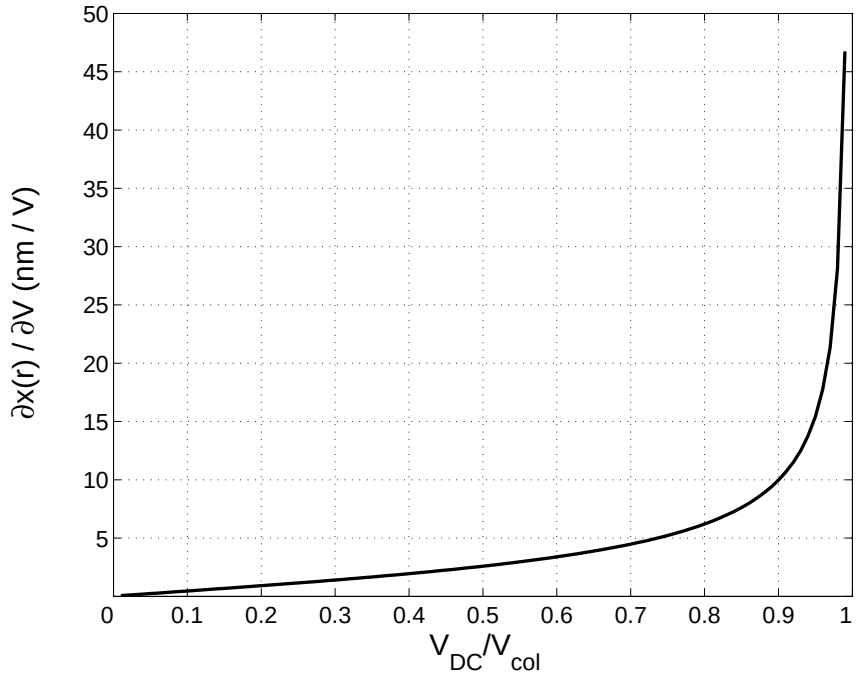

Figure 3.4: The sensitivity of the deflection of a cMUT membrane to the DC voltage changes on the top electrode. The gap height, t_g is 1μm and the collapse voltage, V_{col}= 630 V.

deflection to the DC voltage changes is seen. Thus, small voltage changes result larger membrane deflections when the DC bias is close to the collapse voltage. In this case the approximation used in turns ratio calculations fails. In the computer simulations conducted in this work, the DC bias is taken to be the 90% of the collapse voltage, at which the sensitivity is close to linear region. Since our analysis ignores the effect of the sensitivity at the operating region, the turns ratio values calculated are 5-10% smaller than the actual value.

3.4 Mechanical Impedance

The differential equation governing the deflection of the membrane is written by Mason [27] as;

$$\frac{(Y_0 + T)t_m^3}{12(1-\sigma^2)}\nabla^4 x - t_m T \nabla^2 x - P + t_m \rho \frac{\partial^2 x}{\partial t^2} = 0 \tag{3.11}$$

where, Y_0 is the Young's modulus, T is the residual stress, P is the applied pressure, σ is the Poisson's ratio, ρ is the density of the membrane material and x is the membrane deflection.

Assuming the membrane is clamped at both ends the deflection profile of the membrane under constant uniform pressure is calculated as in [10];

$$x(r) = \frac{P}{\omega^2 t_m \rho}\left[\frac{k_1 J_1(k_1 a)J_0(k_2 r) - k_2 J_0(k_1 r)J_1(k_2 a)}{k_1 J_{10} - k_2 J_{01}} - 1\right] \tag{3.12}$$

where ω is the radian frequency, $J_{01} = J_0(k_1 a)J_1(k_2 a)$, $J_{10} = J_1(k_1 a)J_0(k_2 a)$, J_0 and J_1 are the zeroth and first-order Bessel functions of the first kind. k_1 and k_2 are given by

$$k_1 = \sqrt{\frac{\sqrt{d^2 + 4c\omega^2} - d}{2c}} \text{ and } k_2 = \sqrt{\frac{\sqrt{d^2 + 4c\omega^2} + d}{2c}} \tag{3.13}$$

where

$$c = \frac{(Y_0 + T)t_m^2}{12\rho(1-\sigma^2)} \quad \text{and} \quad d = \frac{T}{\rho} \tag{3.14}$$

The mechanical impedance of a membrane is defined as the ratio of the applied uniform pressure on the membrane to the corresponding velocity of the membrane [14]. The lumped membrane velocity under a harmonic excitation is calculated as [10];

$$v(\omega) = j\omega 2\pi \int_0^a r x(r) dr. \tag{3.15}$$

Using Eq. 3.12 and 3.15, the mechanical impedance, Z_m is calculated to be

$$Z_m = \frac{P}{v} = \frac{jw\rho t_m a k_1 k_2 (k_1 J_{10} - k_2 J_{01})}{a k_1 k_2 (k_1 J_{10} - k_2 J_{01}) - 2(k_1^2 + k_2^2) J_{11}} \tag{3.16}$$

where $J_{11} = J_1(k_1 a)J_1(k_2 a)$.

3.5 Resonance Frequency

Around its first natural resonance frequency of the membrane, Z_m can be modelled by a mass and a spring system. In the equivalent circuit the mass is modelled by an

inductor, L, where the spring is modelled by a capacitor as $1/C$ near the resonance frequency. Thus the mechanical resonance is related to the electrical resonance by the following relation;

$$\omega_r = \sqrt{\frac{\kappa}{m_e}} = \sqrt{\frac{1}{LC}} \tag{3.17}$$

where κ is the stiffness and m_e is the effective mass of the membrane.

Using the electrical equivalent of the resonance behavior, effective mass can be calculated. Near the resonance frequency, the electrical impedance is;

$$Z_m = j\omega L + \frac{1}{j\omega C} \tag{3.18}$$

$$Z_m = j\left(\omega L - \frac{1}{\omega C}\right) \tag{3.19}$$

$$\frac{\partial Z_m}{\partial \omega} = j\left(L + \frac{1}{C\omega^2}\right) \tag{3.20}$$

If we insert the value of ω_r from Eq. 3.17;

$$\left.\frac{\partial Z_m}{\partial \omega}\right|_{\omega_r} = j\left(L + \frac{LC}{C}\right) \tag{3.21}$$

$$\left.\frac{\partial Z_m}{\partial \omega}\right|_{\omega_r} = j2L \tag{3.22}$$

$$\left.\frac{\partial Z_m}{\partial f}\right|_{f_r} = j4\pi m_e \tag{3.23}$$

The effective mass, m_e, can be related to the actual mass of the membrane using the slope of Z_m in Eq. 3.23 as

$$m_e \simeq 1.8\rho t_m \pi a^2. \tag{3.24}$$

The first natural resonance frequency can be written in terms of the effective mass, m_e, and the stiffness, κ, [14] of the membrane as

$$f_r = \frac{1}{2\pi}\sqrt{\frac{\kappa}{m_e}} = \frac{1}{2\pi}\sqrt{\frac{16\pi(Y_0+T)t_m^3}{(1-\sigma^2)a^2}\frac{1}{1.8\rho t_m \pi a^2}} =$$

$$f_r = \frac{2t_m}{\pi a^2}\sqrt{\frac{Y_0+T}{1.8\rho(1-\sigma^2)}} \tag{3.25}$$

The derivations above are based on a membrane with its ends are clamped to the stand. In the FEM analysis the same boundary conditions are applied. However, in an actual cMUT the ends are not clamped to the stand region. Thus, our FEM and lumped model simulations calculate the resonance frequency slightly more than the actual resonance frequency of a cMUT.

It is shown in [28] that the effect of liquid loading in a liquid immersed cMUT is not negligible, especially if the membrane is thin. With liquid loading, the resonance frequency shifts to lower frequencies. Nevertheless, we ignored this effect for the sake of simplicity.

We checked the validity of the model by comparing it with the experimental results of [31]. They measured f_r=12 MHz with a 12 MHz bandwidth. Our predictions for the same geometry[1] and with material constants given in Table C.1 in Appendix C are as follows: f_r=13.1 MHz, bandwidth=13.7 MHz (2.3 MHz to 16 MHz), one-way conversion loss=13.2 dB. The response of the simulated transducers is seen in Fig. 3.5.

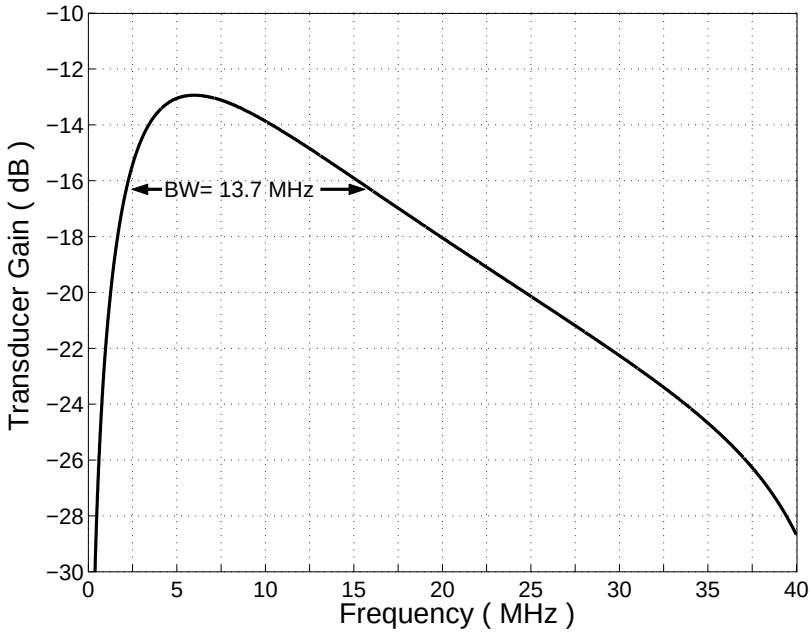

Figure 3.5: The transducer gain v.s. frequency of a transducer with a=18 μm, t_m=0.88 μm, t_g=0.12 μm, t_i=0.2 μm, T=0, R_S=220 kΩ.

[1] a=18 μm, t_m=0.88 μm, t_g=0.12 μm, t_i=0.2 μm, T=0, R_S=220 kΩ

Chapter 4

Optimization of Performance

If the membrane of a cMUT is very thin, the mechanical impedance, Z_m, of the membrane is very low compared to the acoustical impedance of the immersion medium, Z_a, and hence Z_m can be ignored. In this case, the Mason model reduces to just an RC circuit, where bandwidth can be made very large at the expense of gain. In this work, we do not ignore Z_m. We will explore the effect of various device dimensions on the overall circuit. In particular, we would like to optimize the radius (a), the thickness of the membrane (t_m), the gap height (t_g) and the electrical termination resistance (R_S). Z_m and n_c are dependent on the above parameters as it was discussed in Chapter 3. The mechanical termination impedance, Z_aS, is dependent on Z_a as well as the area of the membrane, S. To make a fair comparison of cMUTs with different dimensions, we always choose the maximum applied voltage as $0.9V_{col}$ of the corresponding membrane.

The electrical side termination impedances of cMUTs for transmission and receive modes can be different. Typically, a low resistance electrical source is utilized in the transmission mode. In the receive mode, the optimal electrical termination impedance may be relatively high (10KΩ to 100 KΩ per unit cMUT). Therefore, transmission and receive modes must be treated separately, although cMUT is a reciprocal device.

4.1 Transmit Mode

A cMUT used in transmission mode has a limitation in the applied voltage due to breakdown of insulation material or the collapse voltage of the membrane. Other than this limit, there is no practical limitation in the amount of available electrical power. Moreover, any electrical source resistance can be utilized for exciting the cMUT. Hence, the electrical mismatch between the electrical source and the cMUT is unimportant. In the transmit mode, a large excitation is applied between the zero and V_{col}. It is assumed that a source that can apply this large excitation between the electrodes is assumed to be present. In this case, it is reasonable to try to maximize the pressure at the mechanical side while the maximum allowed voltage is applied at the electrical port. Referring to Fig. 2.1a, let P be the pressure in the immersion medium $P = F/S$ when the applied AC voltage, V_S, is at the maximum

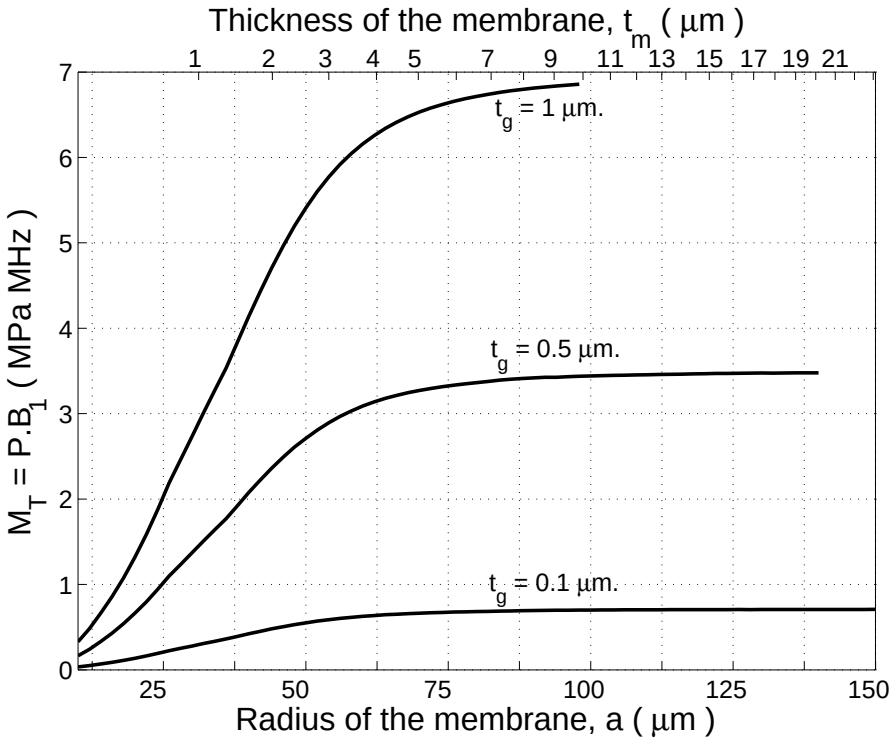

Figure 4.1: Pressure-bandwidth product, M_T, of a cMUT resonating at 5 MHz and operating as a transmitter in water as a function of membrane radius, a, (or as a function of membrane thickness, t_m) for different gap heights. t_m/a^2 is kept constant. The bias voltage is $V_{DC} = 0.45V_{col}$ and the electrical source resistance, R_S is zero.

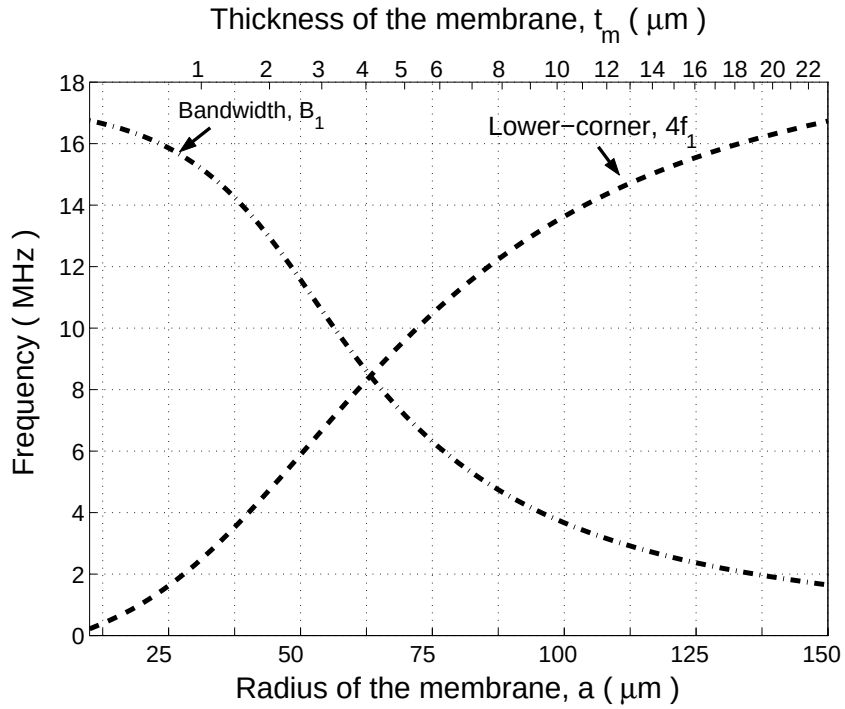

Figure 4.2: Bandwidth (dash-dot), B_1, and lower corner frequency (dashed), f_1, of a cMUT resonating at 5 MHz and operating as a transmitter in water as a function of membrane radius, a, (or as a function of membrane thickness, t_m). t_m/a^2 is kept constant. B_1 and f_1 are independent of t_g. f_1 curve is multiplied by 4 to improve readability. The bias voltage is $V_{DC} = 0.45V_{col}$ and the electrical source resistance, R_S is zero.

allowable value. B_1 is the associated 3-dB bandwidth of the output pressure. In the transmission mode, we define the figure of merit as the pressure-bandwidth product:

$$M_T = PB_1 \tag{4.1}$$

A calculation of M_T is done using the corrected Mason model. If the maximum peak voltage on the electrode is $0.9V_{col}$, n_c is calculated from Eq. 3.10 with $V_{DC} = 0.45V_{col}$. Although the cMUT is highly nonlinear with a large excitation, we treat the problem as if it is linear for simplicity and n_c is assumed to be independent of the applied AC voltage. The resulting M_T is seen in Fig. 4.1 as a function of a or t_m with the gap height, t_g as a parameter. In order to have the same membrane resonance, t_m/a^2 is kept constant as a or t_m is varied.

In Fig. 4.2, the resulting bandwidth, B_1, and 3-dB lower corner frequency, f_1,

are plotted. (3-dB band extends from f_1 to $f_1 + B_1$.)

We see that larger radii (or thicker membranes) give higher pressure-bandwidth products, but smaller bandwidths. For higher bandwidth values, the pressure-bandwidth product must be sacrificed. In other words, large bandwidth values are possible with only very small gain values. In all cases, larger gap heights are preferable, since the corresponding collapse voltages are higher. With a higher applied input voltage, a higher pressure is possible. Bandwidth, B_1 is found to be independent of the gap height.

At the previous results the effect of the spurious capacitances, C_S is ignored. Nevertheless, the results for the transmit mode cMUTs are independent of the shunt input capacitance of the equivalent circuit. Hence, presence of spurious capacitances does not affect the transmission mode results.

4.2 Receive Mode

Unlike the transmission mode where we may have unlimited electrical input power, in receive mode the input acoustic power of the transmitted acoustic signal is limited. It is important to use as much of the available acoustic power as possible. For the best performance the acoustic mismatch at the mechanical side should be minimized. Similarly, the electrical mismatch at the electrical side should be kept at a minimum for good performance. Mismatch loses at both sides are included (Refer to Fig. 2.1b), if we use the *transducer gain*[1] definition;

$$G_T = P_E/P_A \tag{4.2}$$

where P_E is the power delivered to the electrical load resistance, R_S, and P_A is the *available* acoustic power [2] from the immersion medium. The highest transducer gain is obtained if the electrical side impedance of the transducer is conjugately matched to the receiver impedance and the acoustic side impedance of the transducer is equal

[1] See Appendix D

[2] Available power is the power delivered to a load when the load impedance is conjugately matched to the source impedance (Refer to p.610 of [32])

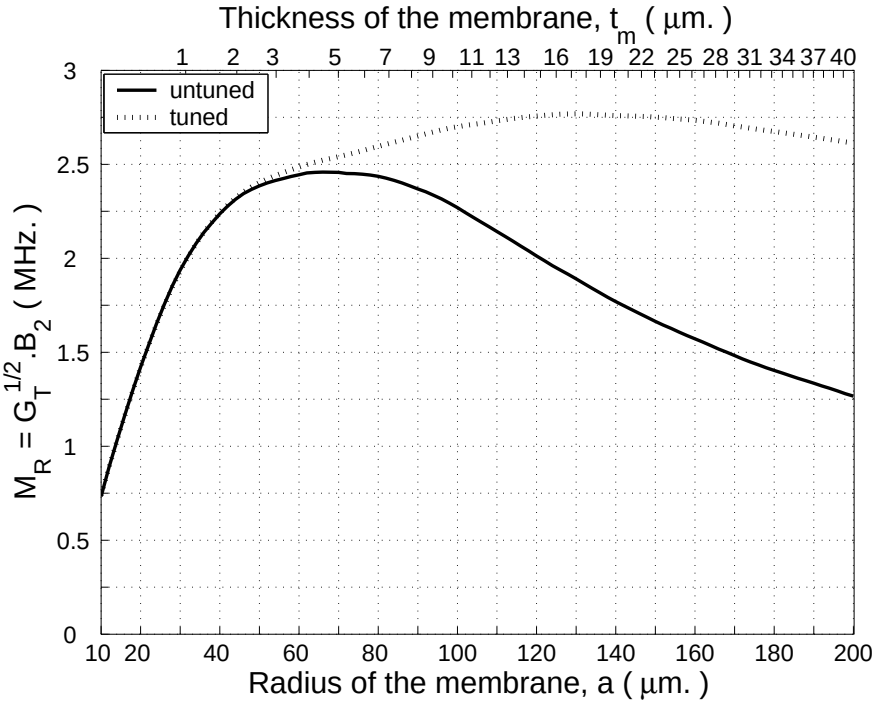

Figure 4.3: Gain-bandwidth product, M_R, of water immersed receiving mode cMUTs resonating at 5 MHz as a function of membrane radius, a, or membrane thickness, t_m, for untuned (solid) and tuned (dotted) cases. t_m/a^2 is kept constant. Electrical termination resistance, R_S is optimal at every point. $V_{DC} = 0.9V_{col}$. The curves are independent of the gap height.

to the acoustic impedance of the immersion medium. Since the transducer gain is a power gain, we define the gain as the square root of the transducer gain and the bandwidth, B_2, as the 3-dB bandwidth of the transducer gain. Hence, in the receive mode we define a figure of merit, M_R, as the gain-bandwidth product:

$$M_R = \sqrt{G_T} B_2 \tag{4.3}$$

In what follows we will investigate the effect of various parameters on this product. We have determined that the gap height does not affect M_R, provided that the cMUT is biased with the same percentage value of the collapse voltage. For all cases we keep the bias voltage at $V_{DC} = 0.9V_{col}$.

We calculated and plotted M_R[3] as a function of a or t_m in Fig. 4.3 for the

[3]Calculation of the transducer power gain is detailed in Appendix D

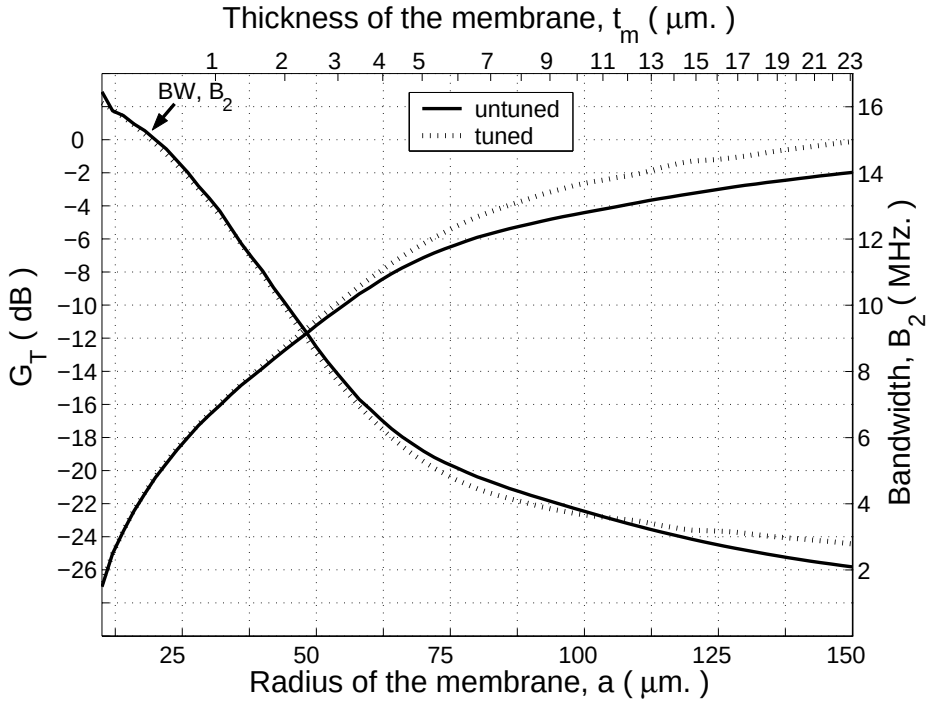

Figure 4.4: Dependence of gain and bandwidth on the membrane radius or thickness for untuned (solid) and tuned (dotted) cMUTs immersed in water and resonating at 5 MHz. R_S is optimal at every point. ($V_{DC} = 0.9V_{col}$) The curves are independent of the gap height.

cMUTs immersed in water. We note that the electrical termination resistance, R_S, is optimally chosen[4] for each $a - t_m$ pair. For the membranes resonating at 5 MHz, the highest gain-bandwidth product is obtained for a=70 μm and t_m=5 μm. If a shunt tuning inductor is added at the electrical port, a further improvement in the gain-bandwidth product is possible as shown in the same figure. The value of this inductor is chosen to maximize the gain-bandwidth product. In this case, a=130 μm, t_m=18 μm and L_T =1.5 μH gives the best M_R.

For small a values, $Z_m S$ is negligible compared to $Z_a S$, and the equivalent circuit may be simplified to an RC circuit. In this case, the tuning does not bring any improvement. But when the mechanical impedance of the membrane is significant, an inductor provides a better match at the electrical port.

The tradeoff between the gain and the bandwidth is demonstrated graphically

[4] R_S value is found by a line search conducted in a range of resistance values. See Appendix B.

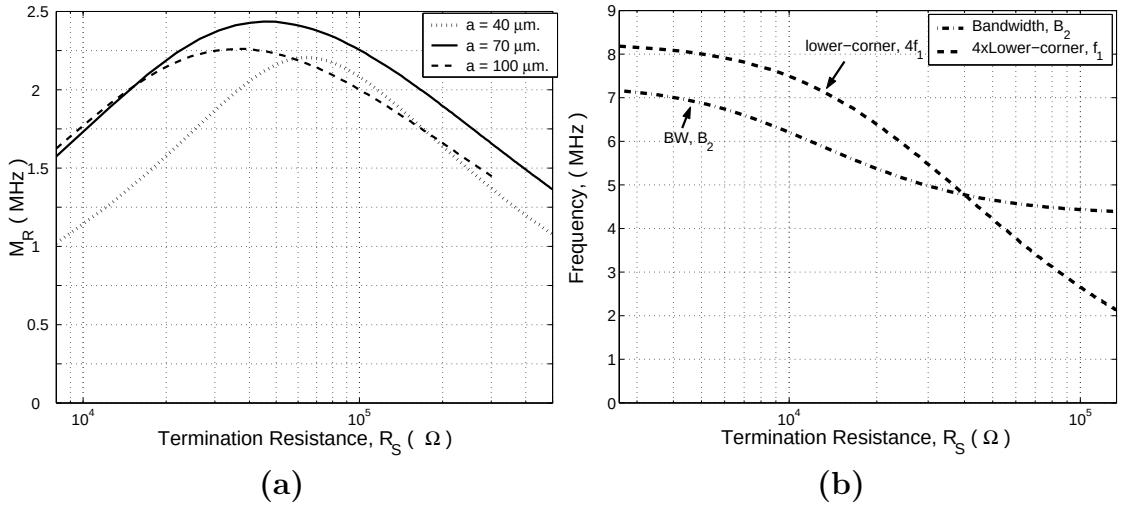

Figure 4.5: **(a)** Gain-bandwidth product, M_R as a function of electrical termination resistance, R_S for different cMUTs resonating at 5 MHz immersed in water. (t_g=0.3 μm, $V_{DC} = 0.9V_{col}$) **(b)** Bandwidth, B_2 (dash-dot) and lower corner frequency, f_1 (dash) of the corresponding cMUT with radius, a=70 μm as a function of R_S.

in Fig. 4.4 as a function of a or t_m. As a goes up, the bandwidth decreases while the gain increases. We note that for each radius value a different membrane thickness is used in such a way to keep the membrane resonance at 5 MHz. In the same figure, the effect of tuning is also indicated. It is clear that adding an inductor does not have a positive effect on the bandwidth, and hence it should be used only when a higher gain is a necessity.

4.2.1 Electrical Termination Resistance, R_S

We demonstrate the effect of the electrical termination resistance on the gain-bandwidth product in Fig. 4.5. It is obvious that there is an optimum R_S value to maximize the gain-bandwidth product. Since n_c depends on the bias voltage, the optimum R_S will be different for different gap heights. We note that in Fig. 4.5a the given R_S is per unit cMUT element. If the actual electrical termination resistance value, R_{Sa}, is lower, we need to connect $N = R_S/R_{Sa}$ many cMUTs in parallel

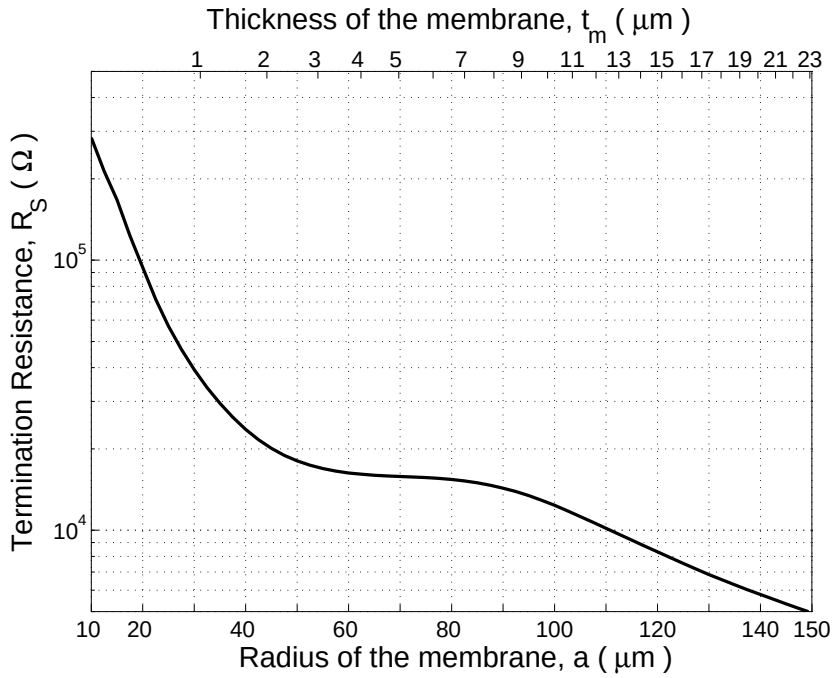

Figure 4.6: The electrical termination resistance, R_S per one receiver cMUT as a function of radius or thickness for untuned cMUTs immersed in water and resonating at 5 MHz. The gap height, t_g=0.1μm. ($V_{DC} = 0.9V_{col}$)

to achieve the desired match. For example, in Fig. 4.5a a cMUT with a=70 μm requires an R_S of approximately 50 kΩ (t_g=0.3μm) for maximum M_R, and if 100 such cMUTs are in parallel, an electrical load of 500 Ω is necessary. Changing the value of R_S is a very simple way of trading gain with bandwidth at the expense of some loss in the gain-bandwidth product. Referring to a=70 μm curve in Fig. 4.5a and Fig. 4.5b, we notice that while R_S is reduced by a factor of five from its optimal value, we lose the gain by a factor of two (6 dB), but the bandwidth can be increased only by 32%.

Note that in Fig. 4.3 and 4.4, the termination resistance R_S is optimally chosen for every other cMUT. The computation of the optimum termination resistance is discussed in Appendix B. In Fig. 4.6, the optimal R_S values as a function of membrane radius are plotted. For the cMUT with the maximum figure of merit, $a = 70\mu$m. and $t_m = 5\mu$m., with the resonance frequency of 5 MHz, the optimal termination resistance is 16 KΩ (t_g=0.1μm.). So for a cMUT array with 320 elements, the electrical termination should be 50Ω.

4.2.2 Acoustical impedance of the medium, Z_a

In the previous sections, we assumed that the cMUTs are operated in water. In this section we explore the effect of the acoustical medium impedance, Z_a on the gain-bandwidth product of the transducers operating in receive mode.

Medium impedance has an effect similar to the electrical termination resistance, R_S, on the gain-bandwidth product. It is seen in Fig. 4.7 that, each cMUT operates best in a specific medium. For example, a transducer with a radius of 70μm, achieves the maximum gain-bandwidth product in Z_a=1.5.10^6 (water). On the other hand, in Fig. 4.3, the cMUT with 70μm radius, is the best cMUT operating in water. Therefore, Fig. 4.7 and Fig. 4.3 define the following relation; each cMUT operates best in a specific medium and in that medium no other cMUT works better.

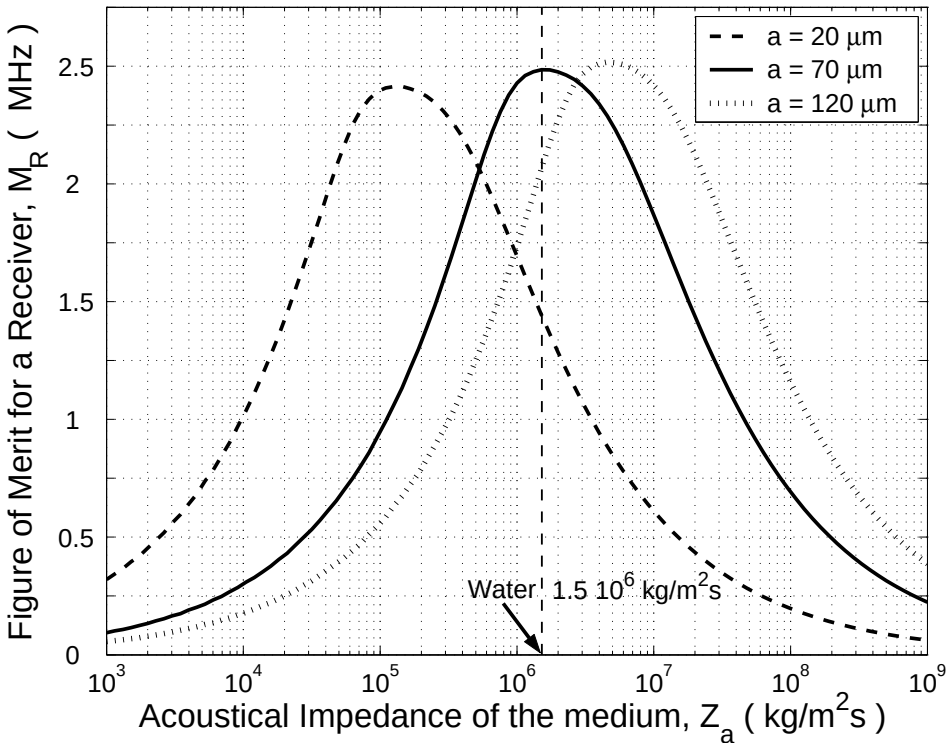

Figure 4.7: Gain-Bandwidth product, M_R as a function of acoustical medium impedance, Z_a for different cMUTs, resonating at 5 MHz. R_S is optimally chosen at every point. The vertical dashed line indicates the acoustical impedance of water (1.5 10^{6}kg/m^{2}s). The gap height, t_g=0.1μm, t_i=0. ($V_{DC} = 0.9V_{col}$)

Referring the previous results, the optimum device dimensions for air-borne applications can be computed (Z_a for air is 415kg/m^{2}s). However the resulting dimensions are impossible to fabricate.

The effect of the spurious capacitances is ignored at the previous calculations of receive mode operation. However, spurious capacitance, C_S affects the results. The figure of merit for the receive mode, M_R decreases with the presence of C_S, nevertheless the location of the optimum transducer does not change. The M_R values for the conditions, with and without C_S are plotted in Fig. 4.8a.

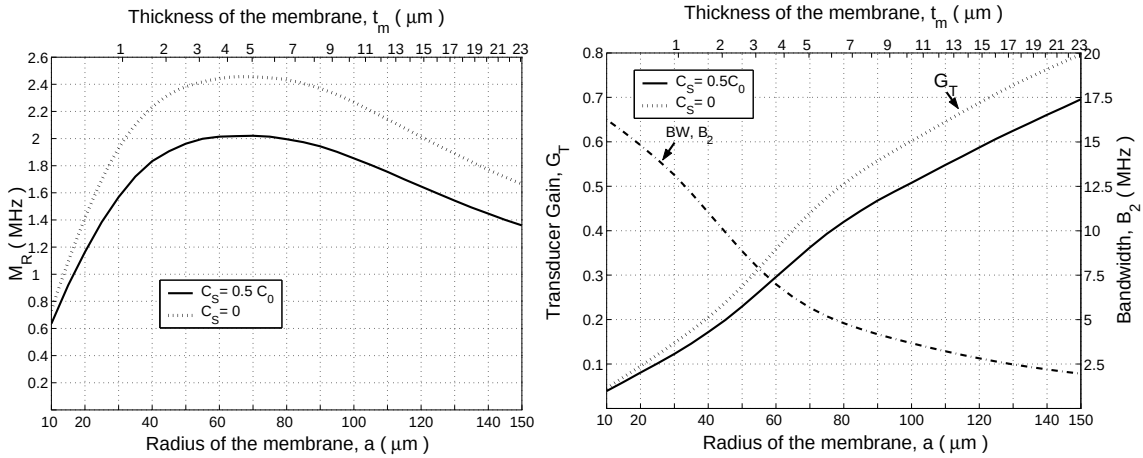

Figure 4.8: **(a)** The figure of merit of a receiver cMUT with spurious capacitance, C_S (dotted) and without C_S (solid) as a function of radius or thickness for untuned cMUTs immersed in water and resonating at 5 MHz. The gap height, t_g=0.1μm. ($V_{DC} = 0.9V_{col}$) **(b)**The gain and the bandwidth of a receiver cMUT with spurious capacitances, C_S (dotted) and without C_S (solid) as a function of radius or thickness for untuned cMUTs immersed in water and resonating at 5 MHz. The gap height, t_g=0.1μm. ($V_{DC} = 0.9V_{col}$)

The presence of C_S does not effect the bandwidth. However the transducer gain decreases. In Fig. 4.8b the transducer gain is plotted with and without spurious capacitances. The reason for the drop of figure of merit, when spurious capacitance is present, is the decrease in the transducer gain. The bandwidth of a transducer is also plotted in Fig. 4.8b. The dashed-dotted curve is common for the two situations.

4.3 Pulse-Echo Mode

In most applications the same transducer is used for both transmission and receive and it is operated in the pulse-echo mode. A transmit-receive switch connects either the transmitter amplifier or the receiver circuit to the electrical side of the cMUT depending on the mode of operation. Hence, the electrical termination resistance, R_S, can be different for transmit and receive modes. In this case, a figure of merit can be defined as

$$M_{PE} = P\sqrt{G_T}B_3 \tag{4.4}$$

where P is defined as in Eq. 4.1, G_T is defined as in Eq. 4.2 and B_3 is the 3-dB bandwidth of the $P\sqrt{G_T}$ product. M_{PE} of the cMUTs with f_r =5 MHz is plotted in Fig. 4.9 for different gap heights.

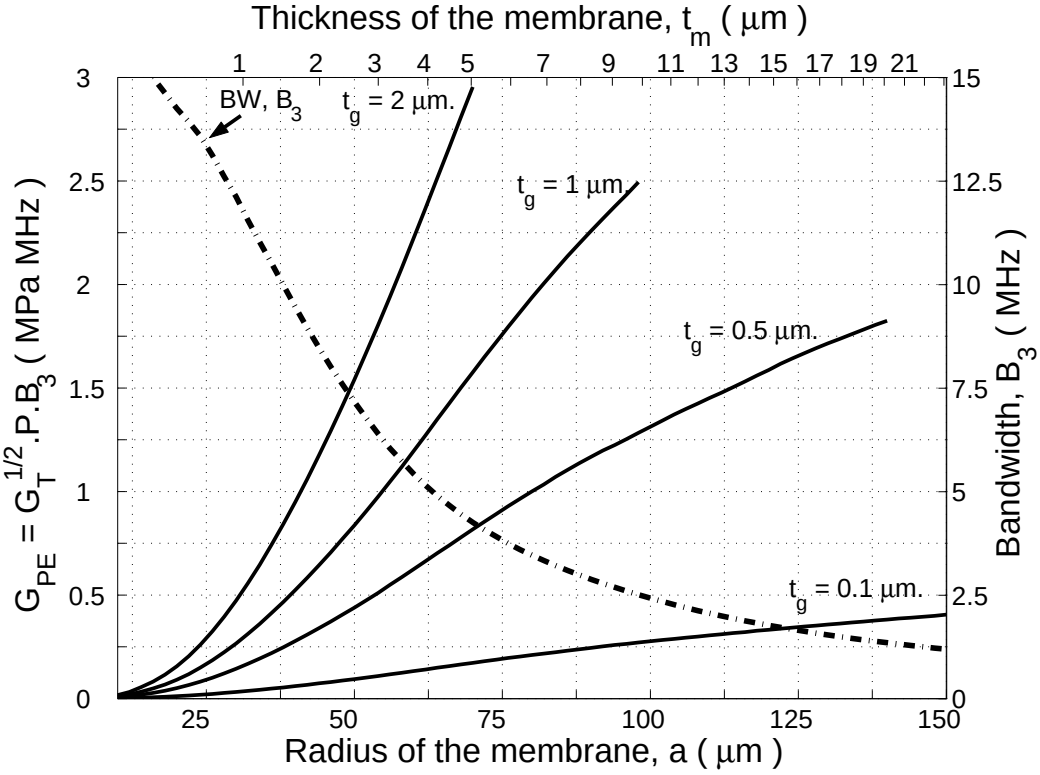

Figure 4.9: Gain-bandwidth product (solid), M_{PE}, and bandwidth (dash-dot), B_3, of water immersed cMUTs with uniform membranes in pulse-echo mode (f_r =5 MHz) for different gap heights. Bandwidth is independent of the gap height.

Chapter 5

Design Graphs

In what follows, we will present normalized versions of the graphs which can be used as design tools for cMUTs with silicon nitride membranes. A number of examples are given to demonstrate the use of these graphs.

5.1 Collapse Voltage

In many applications there is a limit in the operating voltage of the transducers. This is either because of the limits of the electronic circuitry used in the device or because of the breakdown limitations of the device. In either case the collapse voltage of the device should be selected as a design parameter.

The collapse voltage can be calculated approximately by hand calculations using Eq. 5.1, which is repeated here as;

$$V_{col} \simeq 0.7\sqrt{\frac{128(Y_0+T)t_m^3\bar{t}_g^3}{27\epsilon_0(1-\sigma^2)a^4}} \tag{5.1}$$

where $\bar{t}_g$ is the effective gap height, $\bar{t}_g = t_g + \epsilon_0 t_i/\epsilon$. ϵ_0 and ϵ are the permittivity constants of air and insulator material respectively.

5.2 Transmit Mode

Fig. 5.1, 5.2 and 5.3 are normalized graphs that can be utilized to determine the

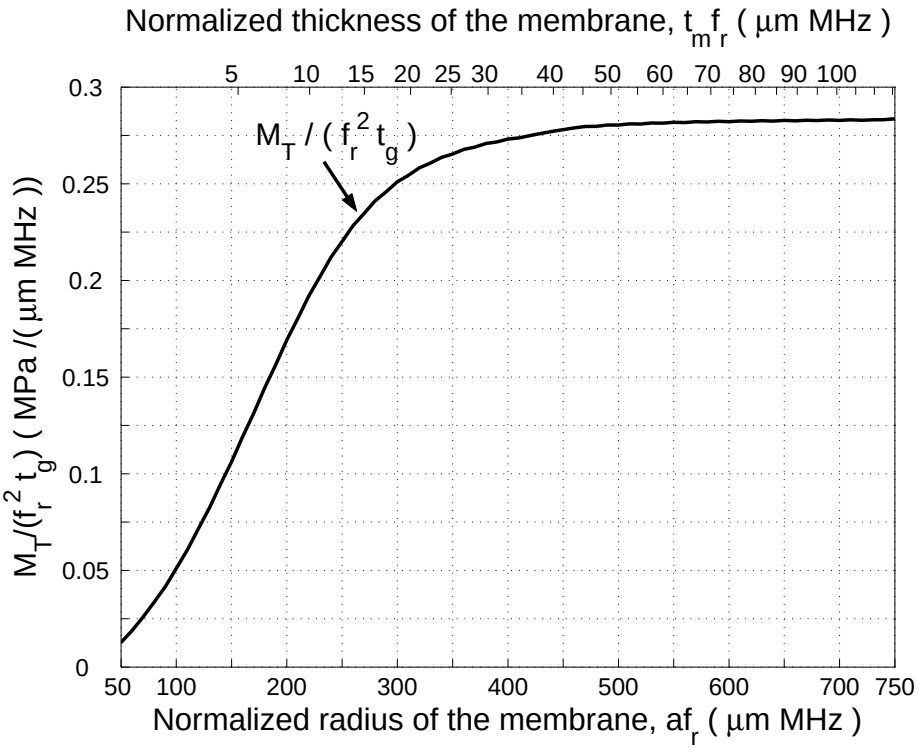

Figure 5.1: Normalized pressure-bandwidth product as a function of normalized membrane radius or thickness for transmitter cMUTs. Bias voltage is at 45% and applied peak-to-peak AC voltage is at 90% of the collapse voltage.

dimensions of a transmitter cMUT at specified frequencies. The first two are essentially same graphs as Fig. 4.1 and 4.2 with its axes normalized with respect to resonance frequency and gap height[1]. Notice that all axes are normalized and their relation with the actual values is provided in the axis labels. Let us demonstrate the use of the graphs by designing a transmitter cMUT to operate between 3-dB frequencies f_1 to f_2 with an output pressure as high as possible. Suppose f_1=3 MHz and f_2=20 MHz. We start at a point with a high M_T such as af_r=300. At this point we read from Fig. 5.2 B_1/f_r=1.83. Since we need a bandwidth of $f_2 - f_1 = B_1$=17 MHz, resonance frequency should be f_r=17/1.83=9.3 MHz. The

[1]Because of the fringe field extension of the radius to $a + \bar{t}_g$ in Eq. 3.4, there is a difficulty of normalization with respect to t_g. However, the graphs remain valid as long as $t_g \ll a$.

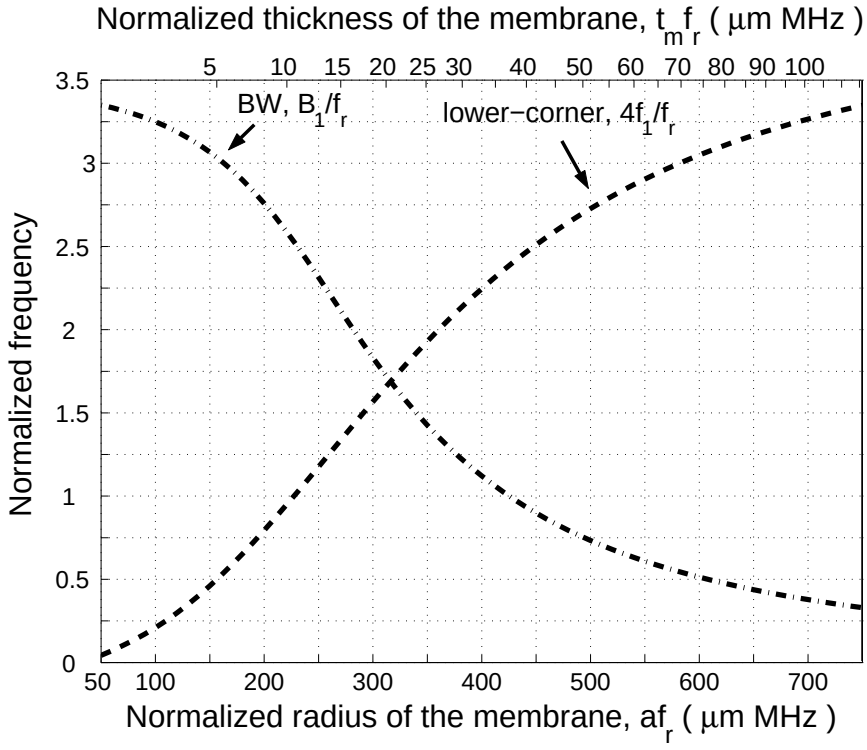

Figure 5.2: Normalized bandwidth (dash-dot) and lower corner frequency (dashed) as a function of normalized membrane radius or thickness for transmitter cMUTs. Bias voltage is at 45% and applied peak-to-peak AC voltage is at 90% of the collapse voltage.

lower corner (f_1) of the band can be determined from Fig. 5.2 as $4f_1/f_r$=1.57 or f_1=3.6 MHz. Since this is larger than the required 3 MHz, we need more iterations. af_r=285 gives satisfactory results. We find f_r=17/2.02=8.4 MHz, f_1=8.42×1.41/4=2.97 MHz and a=34 μm. We determine from the upper x-axis of Fig. 5.2 $t_m f_r$=17 or t_m=17/8.4=2 μm. We should pick a collapse voltage as high as possible. Let V_{col}=150 V. Eq. 5.1 gives nearly the same result as the method in [12]: $\bar{t}_g$ should be 0.35 μm. To make sure that 150 V does not cause a breakdown of the nitride stand, we calculate the E-field: 150/0.35=428 V/μm which is well below the breakdown voltage. Pressure-bandwidth product, M_T, is determined from Fig. 5.1 as M_T=0.24×8.4^2×0.35=5.93 MPaMHz. Hence the output pressure corresponding to an excitation voltage of $0.9\times150 = 135V$ peak-to-peak is P=5.93/17=0.35 MPa. To verify results we performed FEM simulations of the same structure resulting in f_1=2.8 MHz, B_1=16 MHz, V_{col}=153 V, P=0.33 MPa and M_T=5.37.

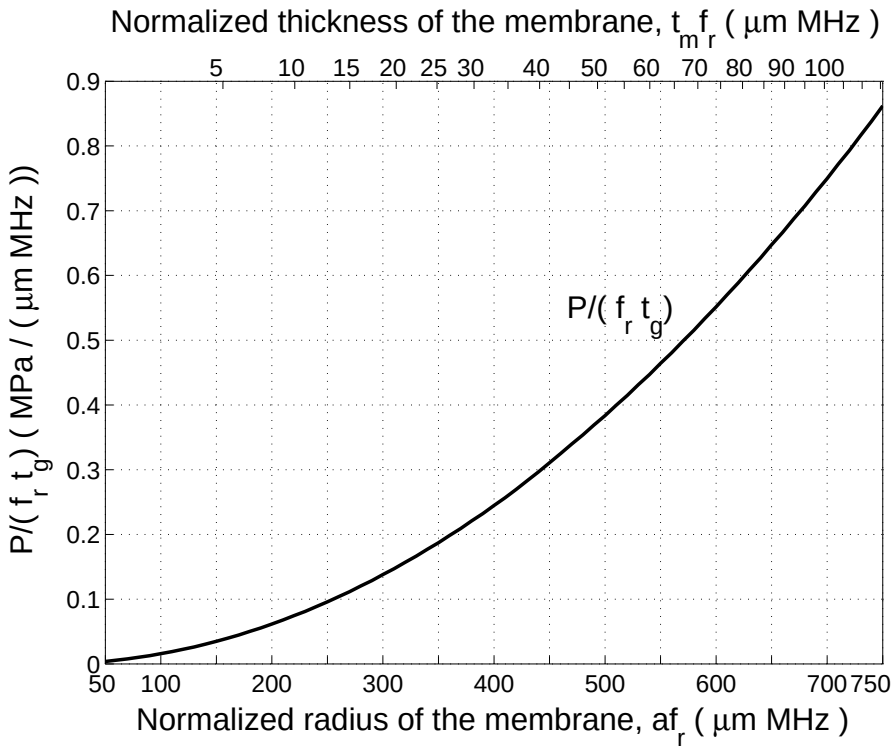

Figure 5.3: Normalized pressure as a function of normalized membrane radius or thickness for transmitter cMUTs. Bias voltage is at 45% and applied peak-to-peak AC voltage is at 90% of the collapse voltage.

As a second example, suppose we need a cMUT with an output pressure of P=0.5 MPa at a center frequency of 8 MHz. Let us determine the dimensions. With a reasonable of gap height of t_g=0.2 μm and f_r=8 MHz we find $P/(f_r t_g)$=0.5/(8×0.2)=0.32 and from Fig. 5.3 we determine af_r=450 and $t_m f_r$=42 or a=56 μm and t_m=5.2 μm. We estimate V_{col}=101 V from Eq. 5.1. From Fig. 5.2 we find the bandwidth B_1=0.8×8=6.4 MHz and f_1=2.5×8/4=5 MHz. Hence, the center frequency is at 5+6.4/2=8.2 MHz. FEM simulations for the given parameters produce f_1=4.6 MHz, B_1=7.2 MHz, V_{col}=109 V and P=0.48 MPa.

5.3 Receive Mode

Normalized graphs to design receiving mode cMUTs are shown in Fig. 5.4, 5.5 and 5.6. There is no tuning inductance, but the electrical load resistance, R_S, is chosen

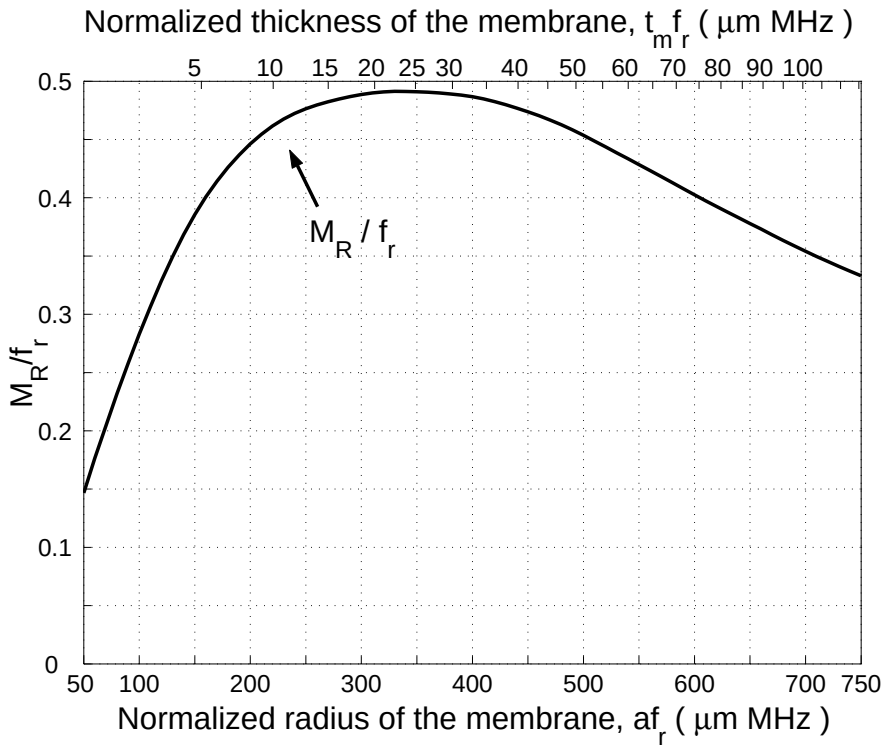

Figure 5.4: Normalized gain-bandwidth product as a function of normalized membrane radius or thickness for receiver cMUTs without tuning. The curve is independent of the gap height.

at the value to maximize the gain-bandwidth product. The missing parameter for designing a transducer for receive mode is the termination resistance. In other words the number of cMUTs in an element for a given characteristic impedance. Fig. 5.7 is a normalized graph that summarizes the R_S values for different resonance frequencies and gap heights.

As an example of use of these graphs, suppose we need a receiver cMUT with B_2=14 MHz of bandwidth between f_1=1 MHz and f_2=15 MHz 3 dB corner frequencies. At af_r=350, we read B_2/f_r=1.12 from Fig. 5.5 and determine f_r = 12.5 MHz. For this choice, we use the f_1 curve in Fig. 5.5 and find $5f_1/f_r$=1.73. So, we calculate f_1 = 4.3 MHz, which does not satisfy our requirement of 1 MHz for the lower end frequency. After a few iterations we find that af_r=200 and f_r=6.4 MHz give satisfactory results. Hence a=31.5 μm and t_m=8.3/6.4=1.3 μm. The gain-bandwidth product is determined from Fig. 5.4 as M_R/f_r=0.44 or M_R=2.8 MHz. Therefore,

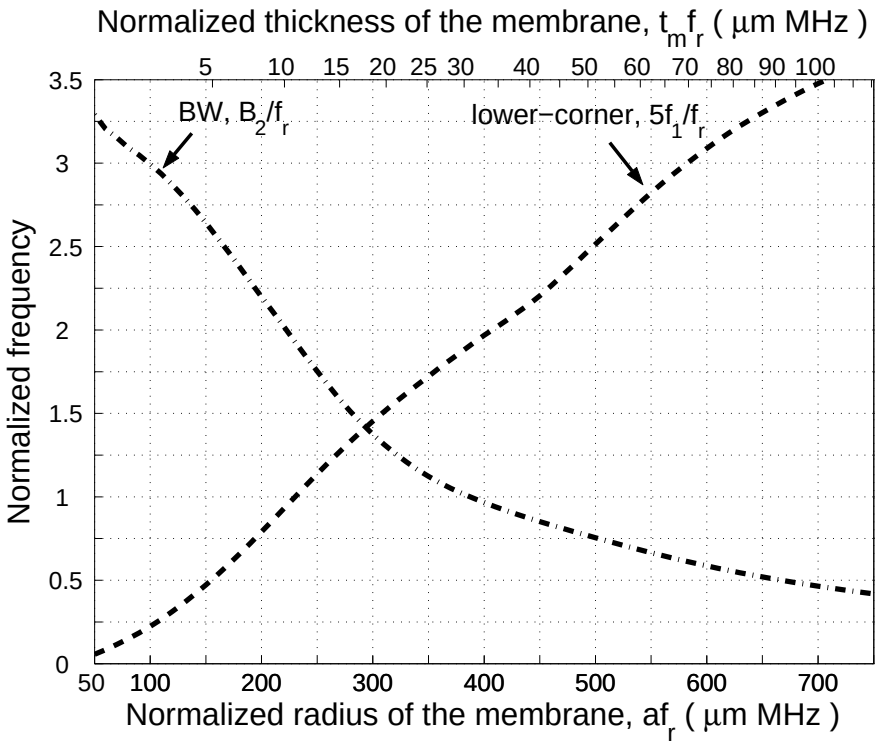

Figure 5.5: Normalized bandwidth (dash-dot) and lower corner frequency (dashed) as a function of normalized membrane radius or thickness for receiver cMUTs without tuning. The curves are independent of the gap height.

the transducer power gain of the cMUT is $\sqrt{G_T}$=2.8/14=0.2=−14 dB. The gap height does not affect the performance and it should be chosen to give an acceptable bias voltage. For example, t_g=0.3 μm gives V_{col}=74 V (Eq. 5.1). In this case the termination resistance for one cMUT is calculated from Fig. 5.7 as 80KΩ. If the actual termination is 500Ω, then 160 cells should be fabricated in one element. At this point the designer should keep in mind the area considerations and pick the real termination resistance accordingly. FEM simulations of the cMUT with the dimensions above give a bandwidth of 13.7 MHz starting at f_1=940 KHz with V_{col}=76 V and G_T=−13.4 dB verifying the predicted gain and bandwidth values.

As a further example suppose we need to design a cMUT with a transducer gain of −3 dB centered at 10 MHz. From Fig. 5.6 we find af_r=610 μmMHz or $t_m f_r$=75 μmMHz satisfies the gain requirement. We also find from Fig. 5.5 B_2/f_r=0.6 and $5f_1/f_r$=3.1. To make $f_1 + B_2/2$=10 MHz we set $3.1f_r/5 +$

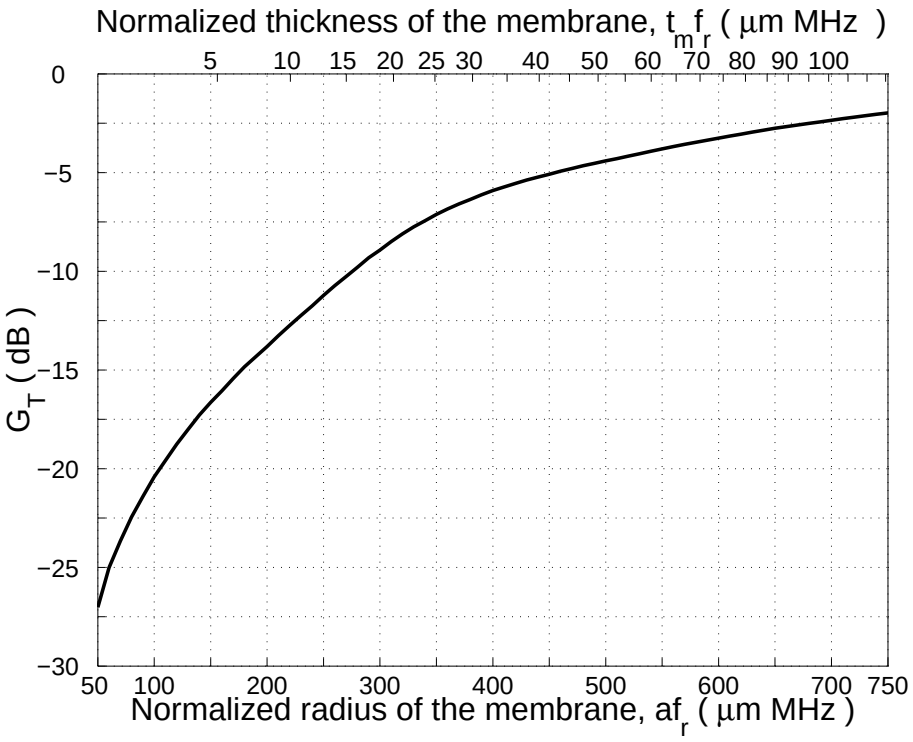

Figure 5.6: Normalized transducer gain as a function of normalized membrane radius or thickness for receiver cMUTs without tuning.

$0.6f_r/2$=10 MHz or f_r=10.9 MHz, f_1=6.7 MHz, B_2=6.5 MHz. Hence, a=56 μm and t_m=6.9 μm. Since this is a rather thick membrane, the gap should be very small to give an acceptable collapse voltage. For t_g=0.1 μm we find V_{col}=57 V ((Eq. 5.1)). The termination resistance, R_S for one cMUT element is calculated as 17KΩ from Fig. 5.7. On the other hand, the values determined from FEM are: f_1=5.7 MHz, B_2=6.5 MHz, V_{col}=65 V, G_T=−2.8 dB.

5.4 Pulse-Echo Mode

Fig. 5.8 and 5.9 are also normalized graphs that can be used to design cMUTs in pulse-echo mode in a similar manner. Inspection of the first graph shows that one should prefer larger gap heights for the best figure of merit. Although a larger membrane radius gives a better merit figure, it results in a smaller bandwidth. As an

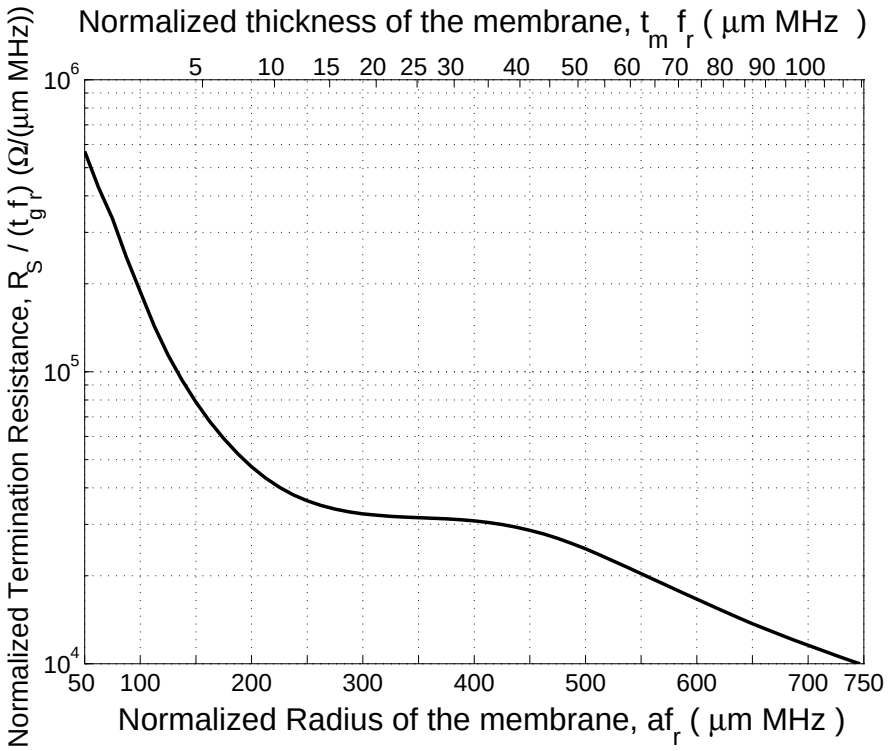

Figure 5.7: Normalized termination resistance, R_S as a function of normalized membrane radius or thickness for receiver cMUTs without tuning. Bias voltage for receive is at 90% of the collapse voltage.

example, we design a transducer with an overall bandwidth of B_3=14 MHz between 3-dB corner frequencies of 1 MHz and 15 MHz. We find from Fig. 5.9 by iteration at $af_r = 160$ μmMHz, B_3=2.3f_r and f_1=0.7f_r/4, resulting in f_r=14/2.3=6 MHz and f_1=1 MHz. Hence, $a = 160/6 = 27$ μm, $t_m = 5.2/6 = 0.9$ μm are determined. If $V_{col} = 50V$, we find from Eq. 5.1 that $\bar{t}_g$=0.27 μm. In transmitter mode we find from Fig. 5.2 B_1=18 MHz and from Fig. 5.3 P=0.065 MPa. In receive mode we use Fig. 5.5 to find B_2=16 MHz and Fig. 5.6 to find $G_T = -16$ dB.

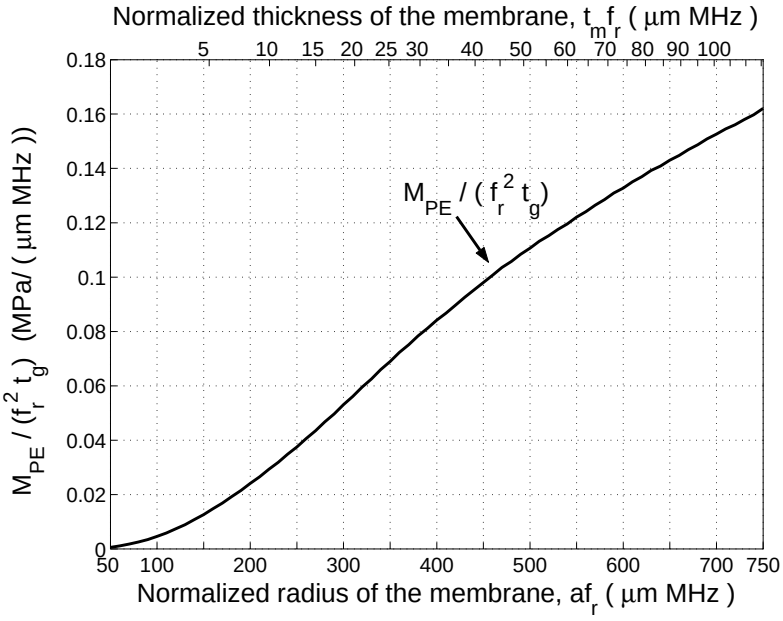

Figure 5.8: Normalized pressure-gain-bandwidth product as a function of normalized membrane radius or thickness for cMUTs in pulse-echo mode. Bias voltage for transmit is at 45% and applied peak-to-peak AC voltage is at 90% of the collapse voltage. Bias voltage for receive is at 90% of the collapse voltage.

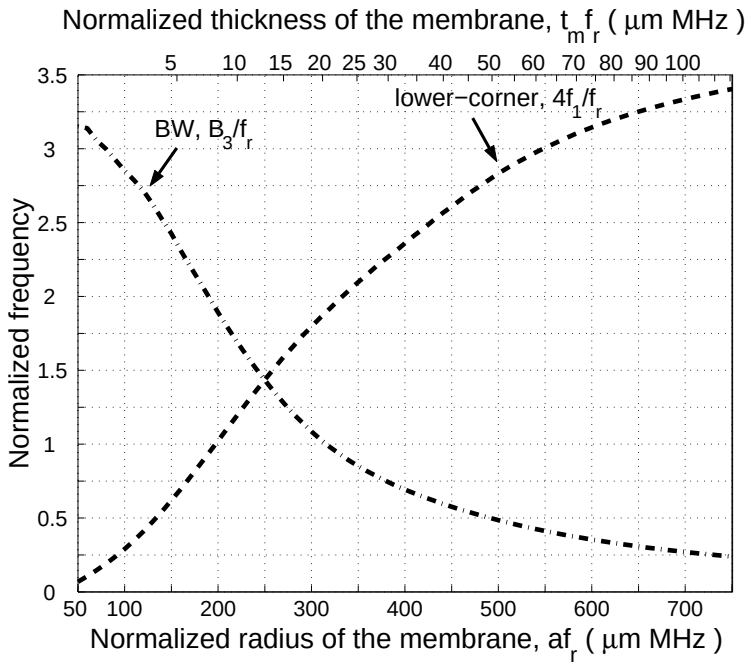

Figure 5.9: Normalized overall bandwidth (dash-dot), and lower corner frequency (dashed) as a function of normalized membrane radius or thickness for cMUTs in pulse-echo mode.

Chapter 6

Conclusions

We defined performance measures for cMUTs in transmit, receive and pulse-echo modes and described the ways of determining the optimum dimensions. In transmit and pulse-echo modes, cMUTs with large gaps are preferable, since the collapse voltages are higher and hence higher excitation voltages are possible. In general, there is a tradeoff between bandwidth and gain-bandwidth product. Smaller membrane radii result in higher bandwidth at the expense of reduced gain-bandwidth product. For the cMUTs operating in receive mode, the gap height does not affect the figure of merit if cMUT is biased at the same percentage value of the collapse voltage. There is an optimal value of the membrane radius or thickness and an optimal electrical termination resistance for the highest gain-bandwidth product. One should sacrifice some gain-bandwidth product, if a higher bandwidth is necessary.

In the FEM and MATLAB simulations the effect of the liquid loading is ignored. The acoustical impedance of the medium is assumed to be real. However, in the case of the membranes with small radius, the water column at top of the membrane does not move simultaneously with the membrane and brings an imaginary part to the medium impedance. Since the cMUT devices are operated in parallel the effective area is larger if the transducers are fabricated close enough to each other. In this case this effect is minimum. On the other hand if the membrane area is large, the medium should vibrate with the membrane so that the acoustic wave can propagate into the medium. This additional mass of the medium increases the effective mass

of the membrane and brings a positive imaginary part to the acoustical impedance of the medium. For the case of larger and stiffer membranes with relatively high mass, the effect of water loading is minimum. We did not use any analytical or finite element calculation to take this effect into account.

In addition, the turns ratio values are calculated without taking into account the sensitivity of the membrane to the DC voltage variations. Since we simulate the cMUTs at 90% of the collapse voltage, it is assumed that the sensitivity is relatively small. Thus, the resulting turns ratio values are 5-10% smaller than FEM simulation results.

Note that we did not include the effect of spurious capacitors. The presence of the spurious capacitances decreases the transducer gain at the receive mode and does not affect the bandwidth. However, they have no effect on the performance of a transmitter cMUT.

We introduced design tools to determine approximately the optimum dimensions of the cMUTs with given frequency response. The circuit parameters are calculated using the approximate models. Note that these methods are the lumped approximations of the distributed parameters in the Mason's equivalent circuit. One should use a full FEM analysis including the liquid loading, if more accurate results are desired.

Appendix A

Finite Element Method Simulations of cMUTs

When analytical models fail to explain complex mechanical structures, Finite Element Method (FEM) simulations are employed. In this study the FEM simulations are used in order to increase the accuracy of the analytical model. ANSYS 8.1 is used as the FEM solver. ANSYS is utilized to solve the electrostatic and harmonic problems of the cMUTs. The methods employed in FEM simulations are based on the FEM simulations in [14]. Please refer [14] and [33] for more detailed discussion of the methods utilized in the FEM simulations.

The parameters required for the lumped equivalent circuit of Mason are shunt input capacitance, turns ratio and the mechanical impedance of the membrane. Of course the collapse voltage is also required in order to determine the operating point of the cMUT.

The axisymmetrical elements are used in the ANSYS simulations since a cMUT is an axisymmetrical device. The silicon nitride elements are meshed with rectangles. Triangular elements are used for meshing the gap and medium regions. the gap and the medium regions are meshed with triangles. The boundary constraints are applied to the membrane edges in order to make sure that the membrane ends are clamped, as the analytical derivations assume.

A.1 Static Analysis

A.1.1 Collapse Voltage

In static analyses a macro called "ESSOLVE" is used. This macro calculates the deflection of the membrane under an electrostatic force. But the electrostatic forces change when the membrane deflects. ESSOLVE calculates the deflection and the electrostatic forces iteratively. This way the collapse voltage of the membrane can be calculated. The maximum voltage value that makes the membrane deflection converge is taken to be the collapse voltage.

A.1.2 Input Capacitance

Once the collapse voltage is calculated, the deflection of the membrane is determined at the operating point ($0.9V_{col}$). At this point the electrostatic field can be extracted. The shunt input capacitance is calculated by the Gaussian integral divided by the applied DC bias. For this purpose a subroutine called "CMATRIX" is employed.

A.1.3 Electrostatic Forces

Note that the DC operating point of the cMUT is 90% of the V_{col} and the AC voltage is 1% of V_{col}. Thus the AC force, F_{AC} can be approximately calculated by taking the difference of the electrostatic forces when 90% and 91% of V_{col} is applied on the top electrode. This difference force, F_{AC} will be used in the calculation of mechanical impedance and turns ratio of the transducer.

The force distribution when a uniform pressure applied on the membrane is calculated by the electrostatic analysis. This force distribution will be used in the calculation of the mechanical impedance.

A.2 Harmonic Analysis

Using harmonic analysis the mechanical impedance of the transducer and the turns ratio of the transformer in the equivalent circuit are determined.

A.2.1 Mechanical Impedance

The mechanical impedance of a cMUT is determined by applying a uniform pressure on the membrane at the desired frequency range with zero acoustic load. The force distribution extracted at the static analysis is used in order to apply harmonic uniform pressure on the membrane. The resulting velocity of the membrane is extracted for all frequencies. The mechanical impedance of the membrane is the ratio of the total force on the membrane to the lumped velocity of the membrane. Note that this analysis neglects the effect of medium loading on the membrane.

A.2.2 Turns Ratio

Turns ratio of the transducer is the ratio of the applied harmonic force to the AC voltage applied between electrodes. Note that the DC operating point affects the magnitude of the turns ratio. Therefore we should employ a prestressed analysis. First the membrane is deflected applying 90% of V_{col} on the top electrode. Then the AC force extracted at the static analyses is used to excite the membrane. The resulting lumped velocity is multiplied by mechanical impedance calculated at the previous harmonic analysis. This multiplication results the equivalent force on the membrane. The ratio of the equivalent force to V_{AC} is the turns ratio of the membrane.

Appendix B

Optimization of Termination Resistance, R_S

In receive mode, it is important to match both the electrical and the acoustical ports. That's why the transducer power gain definition was utilized for receive mode. Thus the value of the termination resistance determines the reflection losses at the electrical port. As it is seen in Fig. 4.5 there is an optimum value for R_S. In the receive mode figures, the optimum value of the R_S is assumed to be connected as the termination for all dimensions. The optimum value is calculated with the following routine demonstrated in Fig. B.1.

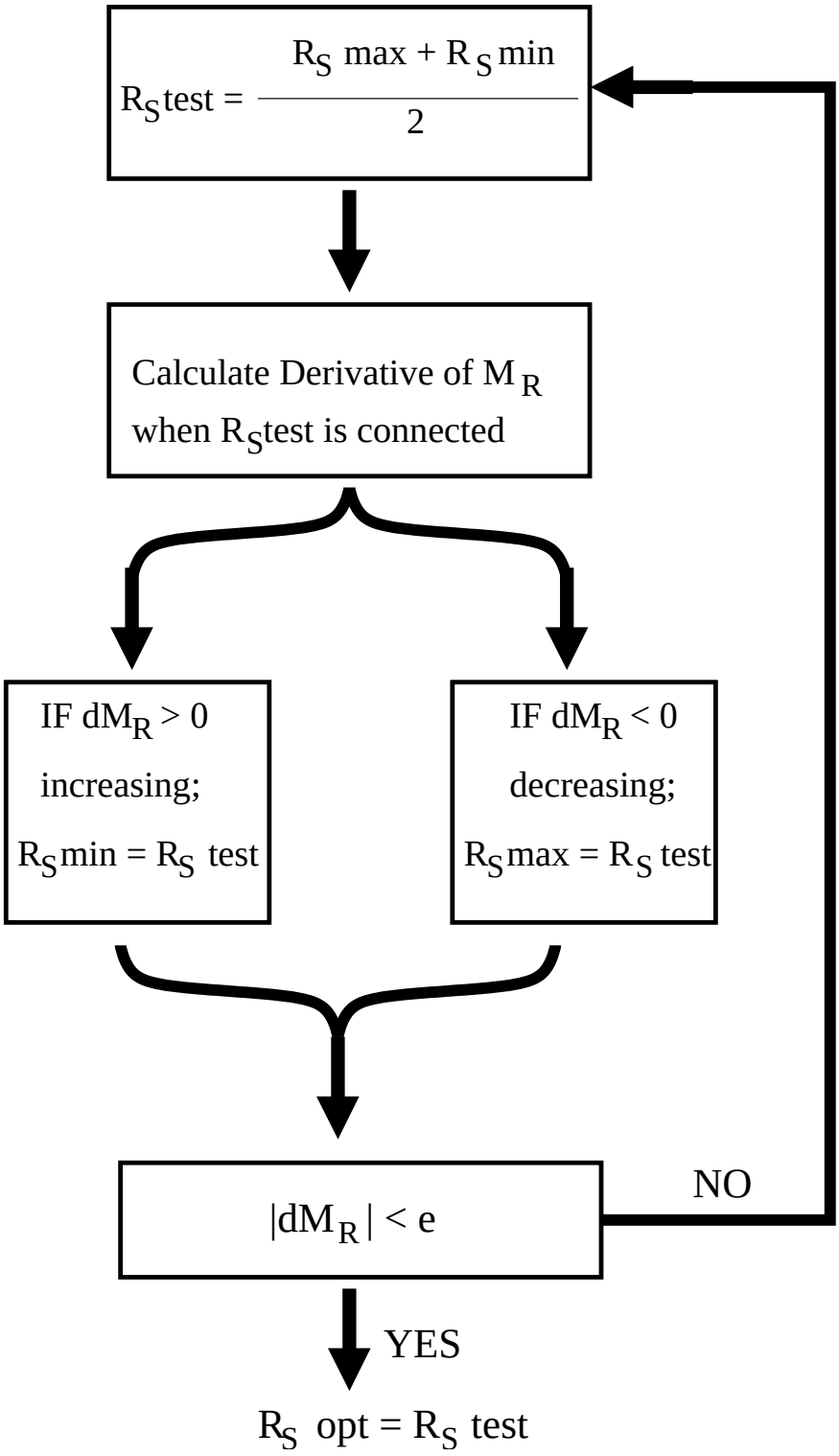

Figure B.1: Flow chart of the termination resistance, R_S optimization routine. The number e, is the tolerance number. Computation stops if the computed derivative is below this value. $R_S max$ and $R_S min$ determine the predefined range that the optimum R_S is searched in.

Appendix C

Constant Parameters

Parameter	Value
Young's Modulus of Si_3N_4, Y_0	3.2×10^5 MPa
Poisson's Ratio of Si_3N_4, σ	0.263
Relative permittivity of Si_3N_4, ϵ_{rn}	5.7
Density of Si_3N_4, ρ	3.27 g/cm^3
Breakdown Voltage of Si_3N_4	900 V/μm

Table C.1: Constant parameters used in the simulations.

Appendix D

Transducer power gain, G_T

The transducer power gain, G_T for Mason's lumped equivalent circuit,

$$G_T = \frac{(1-|\Gamma_L|^2)|s_{21}|^2(1-|\Gamma_S|^2)}{|(1-s_{11}\Gamma_S)(1-s_{22}\Gamma_L)-s_{21}s_{12}\Gamma_L\Gamma_S|^2} \tag{D.1}$$

where s_{11}, s_{12}, s_{21}, s_{22} are the S parameter of the equivalent circuit which are;

$$S = \begin{bmatrix} s_{11} & s_{12} \\ s_{21} & s_{22} \end{bmatrix} = \begin{bmatrix} \frac{A+B/Z_0-CZ_0-D}{A+B/Z_0+CZ_0+D} & \frac{2(AD-BC)}{A+B/Z_0+CZ_0+D} \\ \frac{2}{A+B/Z_0+CZ_0+D} & \frac{-A+B/Z_0-CZ_0+D}{A+B/Z_0+CZ_0+D} \end{bmatrix} \tag{D.2}$$

A, B, C and D are the ABCD parameters of the equivalent circuit, which are;

$$[ABCD] = \begin{bmatrix} A & B \\ C & D \end{bmatrix} = \begin{bmatrix} \frac{1}{n} & Z_m + \frac{n^2}{-jwC_0} \\ \frac{jwC_0}{n} & \frac{Z_m}{n} \end{bmatrix} \tag{D.3}$$

Γ_L and Γ_S are the reflection coefficients of the mechanical and electrical port;

$$\begin{aligned} \Gamma_L &= \frac{Z_aS-Z_0}{Z_aS+Z_0} \\ \Gamma_S &= \frac{R_S-Z_0}{R_S+Z_0} \end{aligned} \tag{D.4}$$

where Z_0 is the reference impedance.

MATLAB is used to evaluate the expressions. Scattering parameters and transducer gain are calculated using the equations given in [32].

Appendix E

MATLAB Simulation codes

E.1 Transmit mode optimization

```
function optim=optimize_t(R,fr,f,tg,ti,opt,Zl)
%Option 1 is electrode on top
%Option 2 is electrode at the bottom
range=length(R); brk=0; freq=1e3:f:3.36e6*fr; for i=1:range

   pair=calc_pair(fr,R(i),tg,opt);%Calculate device dimensions and Capacitance
   V=pair(3);% Collapse voltage
   tm=pair(2);% Membrane thickness
   if  V*0.9 > 900*tg
       brk=1;
       disp('BREAKDOWN occurs in this device.');
   end
   if (tg+ti/5.7+tm/5.7)/3>(3*(tg+ti/5.7)/4) && opt==1
       brk=1;
       disp('Gap error!!')
   end
   if pair(3)==0
       i=range+1;p
       brk=1;
   end
   if brk==0

        [data,C]=calc_parm(R(i),tm,tg,ti,freq,fr,V,opt,0.9); % Calculate electrical parameters
        [c0, n_dc] = calc_cn(R(i),tm,tg,ti,V,opt,0.45);%Calculates turns ratio for 0.45*Vcol

        ZlS=Zl*pi*R(i)^2*1e-12;
```

```
        Fout=abs((0.45*V*n_dc).*(ZlS./(data(:,2)-1./(j*2*pi*data(:,1)*c0)+ZlS)));
        Ac=Fout/(pi*R(i)^2);
        [peak,index]=max(Ac);

        bw_i=find(Ac>(peak*0.707));
        high=data(bw_i(length(bw_i)),1);
        low=data(bw_i(1),1);
        bw=(high-low)/1e6;%(MHz)

        msg=sprintf('Peak Pressure is %g MPa and banwidth is %g MHz',peak,bw);
        disp(msg)
        msg=sprintf('Figure of Merit is %g MPa MHz',peak*bw);
        disp(msg)
        disp('**************************************************************************')
        optim(i,1)=R(i);
        optim(i,2)=max(Ac)*bw;%(MHz uN/V)
        optim(i,3)=max(Ac);%(uN/V)
        optim(i,4)=bw;% MHz.
        optim(i,5)=low/1e6;
    end
end
```

E.2 Receive mode optimization

```
% Author: Selim Olcum, 2004
% This function and its subfunctions executes the gain-bandwidth
% optimization. All the device parameters can be input from the command
% line. This code constitutes the basis for the paper "Optimization of the
% Gain-Bandwidth product of cMUTs".
% Mechanical and electrical parameters are calculated analytically and
% adjusted to fit with the ANSYS results
% All the parameters in the code are in uMKS unit system.
%Option 1 is electrode on top
%Option 2 is electrode at the bottom
function [optim,bwd]=optimize_r(R,fr,f,tg,ti,opt,Zl,tune)

freq=1e3:f:3.36e6*fr;

alfa=0; %%%%%%%%%%%%%%%%%% Water Loading Effect alfa=0.261
range=length(R); brk=0; for i=1:range
   pair=calc_pair(fr,R(i),tg,opt);%Calculate device dimensions and Capacitance
   V=pair(3);%Collapse voltage (V)
   tm=pair(2);%Membrane thickess (um)
   if pair(3)==0
       i=range+1;
       brk=1;
   end
```

```
if brk==0
     [data,C]=calc_parm(R(i),tm,tg,ti,freq,fr,V,opt,0.9); % Calculate electrical parameters

     if tune==0
         peak_gbw=Zs_opt(data,C,R(i),Zl);%Calculate source impedance effect
         [maximum,index]=max(peak_gbw(:,2));
         opt_Zs=peak_gbw(index,1);
         opt_Zs=220000;
         msg=sprintf('Optimum termination resistance is %g K\Omega',opt_Zs/1000);
         disp(msg)
         ZlS=Zl*pi*R(i)^2;% Impedance Data
         [bw,gt]=gain_t(data,C,50e6,ZlS,opt_Zs); % Bandwidth Data
         msg=sprintf('Bandwidth starts at %g MHz and ends at %g MHz.', bw(2)/1e6, bw(3)/1e6);
         disp(msg);
     end

     if tune==1
         peak_gbw=Zs_opt(data,C,R(i),Zl);
         [maximum,index]=max(peak_gbw(:,2));
         opt_Zs=peak_gbw(index,1);
         ZlS=Zl*pi*R(i)^2;% Impedance Data
         [bw,gt]=gain_t(data,C,50e6,ZlS,opt_Zs); % Bandwidth Data
         [maximum,index]=max(gt);
         [opt_Zs,opt_L,gbw]=L_opt(data,C,R(i),Zl,data(index,1),opt_Zs);%Calculate source impedance effect
         msg=sprintf('Optimum termination resistance is %g K \Omega',opt_Zs/1000);
         disp(msg)
         msg=sprintf('Required Inductance L=%g uH.',opt_L*1e18/ceil(opt_Zs/50));
         disp(msg)
         [bw,gt]=tuned_gain(data,C,50e6,ZlS,opt_Zs,opt_L);
     end

     [gain,index]=max(gt);
     msg=sprintf('Peak gain is %g dB at %g MHz. where bandwidth is %g MHz.',gain,data(index,1)/1e6,bw(1)/1e6);
     disp(msg)
     msg=sprintf('Fractional Gain Bandwidth product is %g MHz.',(10^(gain/20))*bw(1)/1e6/fr);
     disp(msg)
     disp('************************************************************')

     gain=max(10.^(gt/20));% Maximum Gain Data
     optim(i,1)=R(i);
     optim(i,2)=gain*bw(1)/1e6;
     optim(i,3)=gain;
     optim(i,4)=bw(1)/1e6;
     optim(i,5)=bw(2);
     optim(i,6)=opt_Zs;

     bwd(i,1)=bw(1);
     bwd(i,2)=bw(2);
     bwd(i,3)=bw(3);
 end
```

```
end
```

E.3 Pulse-echo mode optimization

```
function optim=optimize_p(R,fr,f,tg,ti,opt,Zl)
%Option 1 is electrode on top
%Option 2 is electrode at the bottom
range=length(R); brk=0; freq=1e3:f:3.36e6*fr;

for i=1:range

   pair=calc_pair(fr,R(i),tg,opt);%Calculate device dimensions and Capacitance
   V=pair(3);%Collapse voltage
   tm=pair(2);%Membrane thickess
   if  V*0.9 > 900*tg
       brk=1;
       disp('BREAKDOWN occurs in this device!!!!!!!!!!!!!!!!');
   end
   if pair(3)==0
       i=range+1;p
       brk=1;
   end

   if brk==0
        [data,C]=calc_parm(R(i),tm,tg,ti,freq,fr,V,opt,0.9); % Calculate electrical parameters
        [c0, n_dc] = calc_cn(R(i), tm, tg, ti, V, opt, 0.45);%Calculates turns ratio for 0.45*Vcol

        ZlS=Zl*pi*R(i)^2*1e-12;

        Fout=abs((0.45*V*n_dc).*(ZlS./(data(:,2)-1./(j*2*pi*data(:,1)*c0)+ZlS)));
        Pout=Fout/(pi*R(i)^2);
        msg=sprintf('Output Pressure of the transmitter is %g MPa.',max(Pout));
        disp(msg)

        peak_gbw=Zs_opt(data,C,R(i),Zl);%Calculate source impedance effect
        [maximum,index]=max(peak_gbw(:,2));
        opt_Zs=peak_gbw(index,1);
        msg=sprintf('Optimum termination resistance is %g K\Omega',opt_Zs/1000);
        disp(msg)
        ZlS=Zl*pi*R(i)^2; % Impedance Data
        [bw,gt]=gain_t(data,C,50e6,ZlS,opt_Zs); % Bandwidth Data
        g=(10.^(gt/20));
        V_rec=Pout.*g;
        Ac=V_rec;

        [peak,index]=max(Ac);
        bw_i=find(Ac>(peak*0.707));
        high=data(bw_i(length(bw_i)),1);
```

```
        low=data(bw_i(1),1);
        bw=(high-low)/1e6;%(MHz)

        msg=sprintf('Peak Conversion gain is %g and banwidth is %g',peak,bw);
        disp(msg)
        msg=sprintf('Figure of Merit is %g',max(Ac)*bw);
        disp(msg)
        disp('*********************************************************************')
        optim(i,1)=R(i);
        optim(i,2)=max(Ac)*bw;
        optim(i,3)=max(Ac);
        optim(i,4)=bw;
        optim(i,5)=low;
    end
end
```

E.4 Turns ratio capacitance

```
%   Muhammed N. Senlik - 98027090
%   Modified by Selim Olcum. June 2004
%   Modified by Selim Olcum. November 2004
%   To obtain shunt input capacitance and transformer's ratio at collapse
%          for given membrane radius, thickness, gap height and voltage
%   [co, n] = vdc_find(co, thickness, gap height)
function [co, n] = calc_cn(a, tm, tg, ti, V, opt, perc)

n=100;          % Number of nodes - superpositions -
V=perc*V;       % Operating point is 90% of the collapse Voltage
                % Deflection is about 1/4 of the total effective gap

% Define the material properties of silicon nitride
E = 320E3;      % Young's modulus of silicon nitride (nt / m^2)
sigma = 0.263;  % Poisson's ratio of silicon nitride
ers = 5.7;      % Relative permittivty of silicon nitride
eps0=8.85E-6;   % Permittivity of free space (F / m)
D=E*tm^3/(12*(1-sigma^2));

if opt==1       % Calculation of the effective gap height.
    tgeff=tg+ti/5.7+tm/5.7; % Electrode on top
elseif opt==2
    tgeff=tg+ti/5.7;   % Electrode at the bottom
end

r=1e-6:(a-1e-6)/n:a;            %Initilize integrant
b=1e-6:(a-1e-6)/n:a;            %initilize position of forces
g=ones(1,n+1)*tgeff;            %Initilize the gap effective height
f=zeros(1,n+1);                 %Initilize forces
```

```
% Calculate CO and n for each mesh size

    for k=1:20                  %number of iterations
    w=zeros(1,n+1);
        for j=1:(n+1)             %number of superpositions!!!!!!!!!!!!!!!!!!!!!!!!!!!! Electrode Size
            if j==1
                f(1)=eps0*V^2*pi*b(j)^2/(2*g(j)^2);
            else
                f(j)=eps0*V^2*pi*(b(j)^2-b(j-1)^2)/2/g(j)^2;% Calculation of the discrete force at node bj.
            end
            for i=1:n;           %number of nodes to be calculated
                if r(i)>b(j);
                    w(i)=w(i)+f(j)/(8*pi*D)*((a^2-r(i)^2)*(a^2+b(j)^2)/(2*a^2)+(b(j)^2+r(i)^2)*log(r(i)/a));
                else
                    w(i)=w(i)+f(j)/(8*pi*D)*((a^2+r(i)^2)*(a^2-b(j)^2)/(2*a^2)+(b(j)^2+r(i)^2)*log(b(j)/a));
                end
            end
        end
        iter(k)=max(w);
        g=tgeff-w;
    end

for i=1:(n+1)%!!!!!!!!!!!!!!!Electrode Size
    if i==1
        co_t(i) = pi*r(i)^2*eps0/g(i);
        e_t(i)  = V / g(i);
    else
        co_t(i) = pi*(r(i)^2-r(i-1)^2)*eps0/g(i);
        e_t(i)  = V/g(i);
    end
end
%Here the modification of the fringing fields is made. The radius is
%assumed to be tg larger than its actual value.
co= sum(co_t)+((a+tg)^2-a^2)*pi*eps0*ers/tgeff; n=
sum((e_t+((a+tg)^2-a^2)*pi*eps0*ers/tgeff).*co_t);
```

E.5 Collapse Voltage

```
function V=calc_col(a,tm,tg,opt,ti);

    n=100;                          %Number of nodes
    pl=0;

    Vstr=0;
    Vfin=3000;
    if opt==1
        tgeff=tg+ti/5.7+tm/5.7;
    elseif opt==2
```

```
        tgeff=tg+ti/5.7;
    end

%%%%%%%%%%%%%%%%%%%%%%%%%%%%%%%%%%%%%Constant parameters
    E=3.2e5;
    sigma=0.263;
    eps0=8.85e-6;
    D=E*tm^3/(12*(1-sigma^2));

    converged=0;

    V=(Vfin-Vstr)/2;                %Initialize the applied voltage
    r=1e-6:(a-1e-6)/n:a;            %Initialize integrant
    b=1e-6:(a-1e-6)/n:a;            %initialize position of forces
    g=ones(1,n+1)*tgeff;            %Initialize the gap effective height
    f=zeros(1,n+1);                 %Initialize forces
    k=0;                            %Initialize number of iterations
    maxold=0;                       %Initialize maximum deflection

    while converged==0
        k=k+1;                      %Update iteration number
        w=zeros(1,n+1);             %Initialize deflection array
        for j=2:(n+1)                 %number of superpositions!!!!!!!!!!!!! Electrode Size
            if j==1                 %the force at the center
                f(1)=eps0*V^2*pi*b(j)^2/(2*g(j)^2);
            else
                f(j)=eps0*V^2*pi*(b(j)^2-b(j-1)^2)/2/g(j)^2;%Calculation of the discrete force at node bj.
            end
            for i=1:n               %number of nodes to be calculated
             if r(i)>b(j);       %Outer region
                    w(i)=w(i)+f(j)/(8*pi*D)*((a^2-r(i)^2)*(a^2+b(j)^2)/(2*a^2)+(b(j)^2+r(i)^2)*log(r(i)/a));
                else                %Inner region
                    w(i)=w(i)+f(j)/(8*pi*D)*((a^2+r(i)^2)*(a^2-b(j)^2)/(2*a^2)+(b(j)^2+r(i)^2)*log(b(j)/a));
                end
            end
        end

        iter(k)=max(w);             %Record the maximum deflection
        g=tgeff-w;                  %Update the gap height

        if min(g)<=1e-3
            Vfin=V;                 %If it is collapsed decrease the applied voltage
            Vn=(V+Vstr)/2;
            if pl==1
               subplot(2,1,1)
                plot(iter,'r*')
                subplot(2,1,2)
                plot(diff(iter,2))
                msg=sprintf('Applied Voltage is %d',V);
                title(msg)
```

```
        pause
    end
    V=Vn;                   %Update the applied Voltage
    g=ones(1,n+1)*tgeff;    %Initialize the gap effective height
    k=0;                    %Initialize the iteration number
    clear iter              %Delete the iter array
end

if k>10
    err=abs(max(w)-maxold);     %Calculate the change the deflection
    maxold=max(w);              %Update the old maximum deflection
    if err<1e-3                 %Check if the deflection is converged.
        Vstr=V;                 %If converged change the applied voltage to a larger one.
        Vn=(Vfin+V)/2;

        if abs(V-Vn)<0.1        %Check if the collapse voltage is found
            converged=1;        %If the precision is ok. Stop iterations.
        end
        if pl==1
            subplot(2,1,1)
            plot(iter,'r*')
            subplot(2,1,2)
            plot(diff(iter,2))
            msg=sprintf('Applied Voltage is %d',V);
            title(msg)
            pause
        end
        V=Vn;                   %Update the applied Voltage
        k=0;                    %Initialize the iteration number
        g=ones(1,n+1)*tgeff;    %Initialize the gap effective height
        clear iter              %Delete the iter array
    %%%%%%%%%%%%%%%%%%%%%%%%%%%%Check if the membrane is collapsed
    elseif max(diff(iter,2))>0
        Vfin=V;                 %If it is collapsed decrease the applied voltage
        Vn=(V+Vstr)/2;          %
        if abs(V-Vn)<0.1        %Check if the collapse voltage is found
            converged=1;        %If the precision is ok. Stop iterations.
        end
        if pl==1
            subplot(2,1,1)
            plot(iter,'r*')
            subplot(2,1,2)
            plot(diff(iter,2))
            msg=sprintf('Applied Voltage is %d',V);
            title(msg)
            pause
        end
        V=Vn;                   %Update the applied Voltage
        g=ones(1,n+1)*tgeff;    %Initialize the gap effective height
        k=0;                    %Initialize the iteration number
```

```
            clear iter              %Delete the iter array
        end
    end
end
```

E.6 Gain-Bandwidth Product

```
function gbw=calc_gbw(in,C,Zo,Zs,R,Zl);
% This function takes C in pF, Zo and Zs in Ohms.
% It calculates the Fractional Gain Bandwidth product of a
% particular cMUT with specific source and load impedance

ZlS=Zl*pi*R^2; % Calculate the lumped load impedance. Pa s/m* um^2
[bw,gt]=gain_t(in,C,Zo,ZlS,Zs); % Gain-Bandwidth Data
gbw(1)=max(10.^(gt/20))*bw(1); % Gain bandwidth product
gbw(2)=bw(1); gbw(3)=bw(2);

function gbw=calc_gbwL(in,C,Zo,Zs,R,Zl,L);
% This function takes C in pF, Zo and Zs in Ohms.
% It calculates the Fractional Gain Bandwidth product of a
% particular cMUT with specific source and load impedance

ZlS=Zl*pi*R^2; % Calculate the lumped load impedance.
[bw,gt]=tuned_gain(in,C,Zo,ZlS,Zs,L); % Gain-Bandwidth Data
gbw=(10^(max(gt)/20))*bw(1); % Fractional Gain bandwidth product
```

E.7 Calculate dimensions

```
function pair=calc_pair(fr,R,tg,opt);
% This function calculated the device dimensions for a
% specified resonance frequency and gap height
% It displays the results on the screen
% Function has two options.
    % The first one is to put the electrode on top
    % The second one is to put the electrode at the bottom
% It is modified as it can calculate radius thickness pairs with water
% loading effect included.

% fr is the resonance frequency in Mhz.

pair(1)=R; %The first pair of the parameters is the Radius which is input from the user.

alfa=0; % Alfa is taken to be constant for all cMUT. Since all cMUTs deflects same.
beta=1.8;
rps=(1-(3*pi*alfa/8)^0.714)*R; % Radius of the piston is calculated accordingly.
```

```
%%%%%%%%%%%%%%%%%%%%%%%%%%%%%%%%%%%%%%%%%%%%%%%%%%%%%%%%%%%%%%%%%%%%%%%%%%%%
% Solution for the quadratic relation between the membrane thickness radius
% and frequency.
K=pi*fr^2*1e12*0.931*R^2/(4*3.2e5); mfl=alfa*1000e-18*pi*rps^3;
c(1)=1; c(2)=0; c(3)=-K*beta*3270e-18*pi*R^2; c(4)=-K*mfl;
tm=max(real(roots(c))); pair(2)=tm;
%%%%%%%%%%%%%%%%%%%%%%%%%%%%%%%%%%%%%%%%%%%%%%%%%%%%%%%%%%%%%%%%%%%%%%%%%%%%
pair(3)=calc_col(R,tm,tg,opt,0); V=pair(3);
```

E.8 Electrical Parameters

```
function [data,C]=calc_parm(R,tm,tg,ti,freq,fr,V,opt,perc);
% This function calculated the electrical parameters of a cMUT

Zm = calc_z(freq, R, tm );          % Calculate the lumped  mechanical impedance
%plot(freq,imag(Zm))
%%%%%%%%%%%%%%%%%%%%%%%%%%%%%%%%%% Including the water loading effect;
alfa=0; rps=(1-(3*pi*alfa/8)^0.714)*R;
mfl=j*2*pi*freq*pi*rps^3*alfa*1000e-18; Zm=Zm+mfl;
%%%%%%%%%%%%%%%%%%%%%%%%%%%%%%%%%%%%%%%%%%%%%%%%%%%%%%%%%%%%%%%%%%%%%%%%%%%%
%%%%%%%%%%%%%%%%%%%%%%%%%%%%%%%%%% Calculate the turns ratio and input capacitance
[C, n] = calc_cn(R, tm, tg, ti, V, opt, perc); data=freq';
data(:,2)=Zm.'; data(:,3)=n;
```

E.9 Mechanical Impedance

```
function [Zm] = calc_z(freq, a, tm)
% Calculates lumped mecahnical impedance of the membrane
% a is the full membrane radius

T=0; press=1; Y0      = 320E3; pois    = 0.263; dens    =
3270e-18; w = 2 * pi * freq; r   = 0;
c       = ((Y0 + T) * tm^2)
/ (12 * (1 - pois^2) * dens); d = T / dens; k1  = sqrt((sqrt(d^2 +
4 * c * w.^2)  - d) / (2 * c)); k2  = j * sqrt((sqrt(d^2 + 4 * c *
w.^2)  + d) / (2 * c));

term1    = besselj(0, k1 * r); term2    = besselj(1, k2 * a);
term3    = besselj(0, k2 * r); term4    = besselj(1, k1 * a);
term5    = besselj(0, k1 * a); term6 =  besselj(0, k2 * a);

Zm   = j * (w * dens * tm) .* ((a * k1 .* k2 .* (-k2 .* term5 .*
term2 + k1 .* term4 .* term6)) ./ (a * k1 .* k2 .* (-k2 .* term5
.* term2 + k1 .* term4 .* term6) - 2 * (k1.^2 - k2.^2) .* term4 .*
term2));
```

```
Zm   = j * imag(Zm) * pi * a^2;% lumped mechanical impedance
```

E.10 Transducer gain

```
%Units in this m-file are in uMKS.
function [bw,gt]=gain_t(in,C,z0,ZlS,zs)

z0=z0*1e-12; ZlS=ZlS*1e-12; zs=zs*1e-12;

w=in(:,1); z=in(:,2); n=in(:,3);

Yc=j*2*pi*C*w; z=z+j*(n.^2)./(2*pi*w*C);

a=1./n; b=z./n; c=Yc./n; d=((Yc.*z)./n)+n;

s11=(a+b/z0-c*z0-d)./(a+b/z0+c*z0+d);
s12=2*(a.*d-b.*c)./(a+b/z0+c*z0+d); s21=2./(a+b/z0+c*z0+d);
s22=(-a+b/z0-c*z0+d)./(a+b/z0+c*z0+d);

rl=(ZlS-z0)/(ZlS+z0); rs=(zs-z0)/(zs+z0);

g=((1-(abs(rl))^2).*((abs(s21)).^2).*(1-(abs(rs))^2))./(abs((1-s11*rs).*(1-s22*rl)-s21.*s12*rl*rs)).^2;
gt=10*log10(abs(g));

[peak,index]=max(gt);

bw_i=find(gt>(peak-3)); high=w(bw_i(length(bw_i)));
low=w(bw_i(1));

bw(1)=high-low; bw(2)=low; bw(3)=high;

g=g.^0.5; gt=20*log10(abs(g));
```

E.11 Inductance Optimization

```
function [opt_Zs,opt_L,gbw]=L_opt(in,C,R,Zl,fr,opt_Zs)
opt_L=1/(4*pi^2*fr^2*C); gbwerr=1e6; gbw=0; delta=0.01;
deltar=0.001;
nbr=50;% number of data points
nbrr=20; while abs(gbw-gbwerr)/1e6>0.1
    gbwerr=gbw;
    delta=0.05;
    nbr=50;
    top1=0;
 %************************* Inductance Optimization  ****************************************
```

```
  Le=log10(opt_L);
  start_L=10^(Le*(1-2*delta));
  finish_L=10^(Le*(1+2*delta));
  inc=(finish_L-start_L)/nbr;

  for i=1:nbr+1
      L=start_L+inc*(i-1);
      gbw=calc_gbwL(in,C,50e6,opt_Zs,R,Zl,L);%Black curve
      peak_gbwL(i,2)=gbw;%Value of Maximum gain bandwidth at specific Source impedance
      peak_gbwL(i,1)=L;%Source impedance under test
  end

  [maximum,index]=max(peak_gbwL(:,2));
  opt_L=peak_gbwL(index,1);
%*************************************************************************************************
%************************ Resistance Optimization  ***************************************
  start_zs=opt_Zs/10;
  finish_zs=opt_Zs*10;

  while top1==0;
      inc=0;
      dec=0;
      Zs=(start_zs+finish_zs)/2;
      Zse=log10(Zs);

      gbw=calc_gbwL(in,C,50e6,Zs,R,Zl,opt_L);
      gbwl=calc_gbwL(in,C,50e6,10^(Zse*(1-delta)),R,Zl,opt_L);
      gbwh=calc_gbwL(in,C,50e6,10^(Zse*(1+delta)),R,Zl,opt_L);

      if gbw>gbwh
          dec=1;
      end
      if gbw>gbwl
          inc=1;
      end
      if inc==1 && dec==1
          top1=1;
      elseif inc==1 && dec==0
          start_zs=(start_zs+finish_zs)/2;
      elseif inc==0 && dec==1
          finish_zs=(start_zs+finish_zs)/2;
      else
          delta=delta+deltar;
          nbr=nbr+nbrr;
          disp('Span range is enlarged')
      end
  end

  start_zs=10^(Zse*(1-delta));
  finish_zs=10^(Zse*(1+delta));
```

```
    inc=(finish_zs-start_zs)/nbr;
    for i=1:nbr+1
        Zs=start_zs+inc*(i-1);
        gbw=calc_gbwL(in,C,50e6,Zs,R,Zl,opt_L);%Black curve
        peak_gbw(i,2)=gbw;%Value of Maximum gain bandwidth at specific Source impedance
        peak_gbw(i,1)=Zs;%Source impedance under test
    end
    [maximum,index]=max(peak_gbw(:,2));
    opt_Zs=peak_gbw(index,1);
  %*************************************************************************************************
    gbw=calc_gbwL(in,C,50e6,opt_Zs,R,Zl,opt_L);
end
%First column of peak_bw is the peak gain bandwidth product.
%Second column of peak_bw is the Source impedance value where the gain bandwidth product is maximum
```

E.12 R_S Optimization

```
function peak_gbw=Zs_opt(in,C,R,Zl)
%Zl is the acoustic impedance of the medium in Pa s/m
%C is in pF, R is in um
global peak_gbw; start=0; finish=5e12; top=0; delta=0.1;
deltar=0.002;
nbr=150;% number of data points
nbrr=50; while top==0;
    inc=0;
    dec=0;
    Zs=(start+finish)/2;
    Zse=log10(Zs);
    gbwl=calc_gbw(in,C,50e6,10^(Zse*(1-delta)),R,Zl);%Black curve
    gbw=calc_gbw(in,C,50e6,Zs,R,Zl);%Black curve
    gbwh=calc_gbw(in,C,50e6,10^(Zse*(1+delta)),R,Zl);%Black curve

    if gbw(1)>gbwh(1)
        dec=1;
    end
    if gbw(1)>gbwl(1)
        inc=1;
    end
    if inc==1 && dec==1
        top=1;
    elseif inc==1 && dec==0
        start=(start+finish)/2;
    elseif inc==0 && dec==1
        finish=(start+finish)/2;
    elseif gbwl(1)==0 && gbw(1)==0 && gbwh(1)==0
        finish=finish/2;
```

```
    elseif inc==0 && dec==0
        %disp('Span range is enlarged')
        delta=delta+deltar;
        nbr=nbr+nbrr;
        %start=start/2;
        %finish=finish*2;
    end

end
start=10^(Zse*(1-2*delta)); finish=10^(Zse*(1+2*delta));
inc=(finish-start)/nbr; for i=1:nbr+1
    Zs=start+inc*(i-1);
    gbw=calc_gbw(in,C,50e6,Zs,R,Zl);%Black curve
    peak_gbw(i,2)=gbw(1);%Value of Maximum gain bandwidth at specific Source impedance
    peak_gbw(i,1)=Zs;%Source impedance under test
    peak_gbw(i,3)=gbw(2);
    peak_gbw(i,4)=gbw(3);
end
%First column of peak_bw is the peak gain bandwidth product.
%Second column of peak_bw is the Load impedance value where the gain bandwidth product is maximum
```

E.13 Tuned Transducer Gain

```
%Units in this m-file are in uMKS.
function [bw,gt]=tuned_gain(in,C,z0,ZlS,zs,L) pl=0;

z0=z0*1e-12; ZlS=ZlS*1e-12; zs=zs*1e-12;

w=in(:,1); z=in(:,2); n=in(:,3);

Yc=j*((2*pi*w).^2*L*C-1)./(2*pi*w*L); z=z+j*(n.^2)./(2*pi*w*C);

a=1./n; b=z./n; c=Yc./n; d=((Yc.*z)./n)+n;

s11=(a+b/z0-c*z0-d)./(a+b/z0+c*z0+d);
s12=2*(a.*d-b.*c)./(a+b/z0+c*z0+d); s21=2./(a+b/z0+c*z0+d);
s22=(-a+b/z0-c*z0+d)./(a+b/z0+c*z0+d);

rl=(ZlS-z0)/(ZlS+z0); rs=(zs-z0)/(zs+z0);

g=((1-(abs(rl))^2).*((abs(s21)).^2).*(1-(abs(rs))^2))./(abs((1-s11*rs).*(1-s22*rl)-s21.*s12*rl*rs)).^2;
gt=10*log10(abs(g));
[peak,index]=max(gt); bw_i=find(gt>(peak-3));
high=w(bw_i(length(bw_i))); low=w(bw_i(1)); bw(1)=high-low;
bw(2)=low; bw(3)=high; g=g.^0.5; gt=20*log10(abs(g));
```

Bibliography

[1] H. Soh, I. Ladabaum, A. Atalar, C. Quate, and B. Khuri-Yakub, "Silicon micromachined ultrasonic immersion transducers," Appl. Phys. Lett., vol. 69, pp. 3674–3676, 1996.

[2] I. Ladabaum, X. Jin, H. Soh, F. Pierre, A. Atalar, and B. Khuri-Yakub, "Microfabricated ultrasonic transducers: Towards robust models and immersion devices," in Proc. of 1996 Ultrasonics Symposium, pp. 335–338, 1996.

[3] A. Buhrdorf, O. Ahrens, and J. Binder, "Capacitive micromachined ultrasonic transducers and their application," in Proc. of 2001 Ultrasonics Symposium, pp. 933–940, 2001.

[4] J. McIntosh, D. Hutchins, G. Etcheverry, D. Billson, R. Noble, R. Davies, and L. Koker, "Micromachined capacitive transducer array for imaging in air," in Proc. of 2001 Ultrasonics Symposium, pp. 929–932, 2001.

[5] J. McIntosh, D. Hutchins, D. Billson, T. Robertson, R. Noble, and A. Jones, "The characterization of capacitive micromachined ultrasonic transducers in air.," Ultr., vol. 40, pp. 477–483, 2002.

[6] J. Johnson, O. Oralkan, U. D. A. Ergun, M. Karaman, and B. Khuri-Yakub, "Medical imaging using capacitive micromachined ultrasonic transducer arrays," IEEE Trans. Ultrason., Ferroelect., Freq. Contr., vol. 49, pp. 1321–1329, 2002.

[7] O. Oralkan, A. Ergun, J. Jhonson, M. Karaman, U. Demirci, K. Kaviani, T. Lee, and B. Khuri-Yakub, "Capacitive micromachined ultrasonic transducers: Next generation arrays for acoustic imaging?," in Proc. of 2002 Ultrasonics Symposium, pp. 1596–1610, 2002.

[8] O. Oralkan, A. Ergun, C. Cheng, J. Jhonson, M. Karaman, T. Lee, and B. Khuri-Yakub, "Volumetric ultrasound imaging using 2-D cMUT arrays," in Proc. of 2003 Ultrasonics Symposium, pp. 1581–1594, 2003.

[9] A. Bozkurt, F. Degertekin, A. Atalar, and B. Khuri-Yakub, "Analytic modelling of loss and cross-coupling in capacitive micromachined ultrasonic transducers," in Proc. of 1998 Ultrasonics Symposium, pp. 1025–1028, 1998.

[10] I. Ladabaum, X. Jin, H. Soh, A. Atalar, and B. Khuri-Yakub, "Surface micromachined capacitive ultrasonic transducers," IEEE Trans. Ultrason., Ferroelect., Freq. Contr., vol. 45, pp. 678–690, 1998.

[11] A. Caronti, G. Caliano, A.Iula, and M. Pappalardo, "An accurate model for capacitive micromachined ultrasonic transducers," IEEE Trans. Ultrason., Ferroelect., Freq. Contr., vol. 49, pp. 159–167, 2002.

[12] A. Nikoozadeh, B. Bayram, G. Yaralioglu, and B. Khuri-Yakub, "Analytical calculation of collapse voltage of cMUT membrane," in Proc. of 2004 Ultrasonics Symposium, 2004.

[13] Y. Roh and B. Khuri-Yakub, "Finite element analysis of underwater capacitor micromachined ultrasonic transducers," IEEE Trans. Ultrason., Ferroelect., Freq. Contr., vol. 49, pp. 293–298, 2002.

[14] A. Bozkurt, I. Ladabaum, A. Atalar, and B. Khuri-Yakub, "Theory and analysis electrode size optimization for capacitive microfabricated ultrasonic transducers," IEEE Trans. Ultrason., Ferroelect., Freq. Contr., vol. 46, pp. 1364–1374, 1999.

[15] J. McLean, R. Guldiken, and F. Degertekin, "Cmuts with dual electrode structure for improved transmit and receive performance," in Proc. of 2004 Ultrasonics Symposium, 2004.

[16] B. Bayram, E. Hæggström, G. Yaralioglu, and B. Khuri-Yakub, "A new regime for operating capacitive micromachined ultrasonic transducers," IEEE Trans. Ultrason., Ferroelect., Freq. Contr., vol. 50, pp. 1184–1190, 2003.

[17] B. Khuri-Yakub, C. Cheng, F. Degertekin, S. Ergun, S. Hanse, X. Jin, and O. Oralkan, "Silicon micromachined ultrasonic transducers," Jpn. J. Appl. Phys., vol. 39, pp. 2883–2887, 2000.

[18] Y. Huang, A. S. Ergun, E. Hæggström, M. H. Badi, and B. T. Khuri-Yakub, "Fabricating capacitive micromachined ultrasonic transducers with wafer-bonding," IEEE/ASME Journal of Microelectromechanical Systems, vol. 12, pp. 128–137, 2003.

[19] J. Knight, J. McLean, and F. Degertekin, "Low temperature fabrication of immersion capacitive micromachined ultrasonic transducers on silicon and dielectric substrates," IEEE Trans. Ultrason., Ferroelect., Freq. Contr., vol. 51, pp. 1324–1333, 2004.

[20] A. Buhrdorf, A. Lohfink, S. Junge, P. Eccardt, and W. Benecke, "Fabrication and characterization of a new capacitive micromachined ultrasonic transducer (cmut) using polysilicon as membrane and sacrifical layer material," in Proc. of 2003 Ultrasonics Symposium, pp. 469–472, 2003.

[21] P. Eccardt and K. Niederer, "Micromachined ultrasound transducers with improved coupling factors from a cmos compatible process," Ultr., vol. 38, pp. 774–780, 2000.

[22] D. Memmi, V. Foglietti, E. Cianni, G. Caliano, and M. Pappalardo, "Fabrication of capacitive micromechanical ultrsonic transducers by low-temperature process," Sens. and Actu. A, vol. 99, pp. 85–91, 2002.

[23] D. Greve, J. Neumann, I. Oppenheim, S. Pessiki, and D. Ozevin, "Robust capacitive mems ultrasonic transducers for liquid immersion," in Proc. of 2003 Ultrasonics Symposium, pp. 5–8, 2003.

[24] G. Yaralioglu, M. Badi, A. Ergun, and B. Khuri-Yakub, "Improved equivalent circuit and finite element method modelling of capacitive micromachined ultrasonic transducers," in Proc. of 2003 Ultrasonics Symposium, pp. 469–472, 2003.

[25] M. Haller and B. Khuri-Yakub, "A surface micromachined electrostatic ultrasonic air transducer," in Proc. of 1994 Ultrasonics Symposium, pp. 1241–1244, 1994.

[26] M. Haller and B. Khuri-Yakub, "A surface micromachined electrostatic ultrasonic air transducer," IEEE Trans. Ultrason., Ferroelect., Freq. Contr., vol. 43, pp. 1–6, 1996.

[27] W. Mason, Electromechanical Transducers and Wave Filters. Van Nostrand, New York, 1942.

[28] A. Lohfink, P.-C. Eccardt, W. Benecke, and M. Meixner, "Derivation of a 1D cMUT model from FEM results for linear and nonlinear equivalent circuit simulation," in Proc. of 2003 Ultrasonics Symposium, pp. 465–468, 2003.

[29] G. Yaralioglu, A. Ergun, B. Bayram, E. Hæggström, and B. Khuri-Yakub, "Calculation and measurement od electromechanical coupling coefficient of capacitive micromachined ultrasonic transducers," IEEE Trans. Ultrason., Ferroelect., Freq. Contr., vol. 50, pp. 1951–1954, 2003.

[30] S. Timoshenko and S. Woinowsky-Krieger, Theory of Plates ans Shells. New York: McGraw Hill, 1959.

[31] U. Demirci, J. Johnson, A. Ergun, M. Karaman, and B. Khuri-Yakub, "Capacitive micromachined ultrasonic transducer arrays for medical imaging: Experimental results," in Proc. of 2001 Ultrasonics Symposium, pp. 957–960, 2001.

[32] D. Pozar, Microwave Engineering. New York: John Wiley and Sons, 1998.

[33] A. Bozkurt, Modelling and Characterization of Capacitive Micromachined Ultrasonic Transducers. PhD thesis, Bilkent University, Jan 2000.